

Measurement of eight scalar and dipolar couplings for methine-methylene pairs in proteins and nucleic acids.

Emeric Miclet, Jérôme Boisbouvier, and Ad Bax

SUPPORTING INFORMATION

### Sources of systematic error in coupling measurements with 3D S<sup>3</sup>E HBCBCA

**Cross-correlated relaxation:** Beyond enhancing apparent resolution and thereby improving precision of peak picking, removal of unresolved  ${}^2J_{C\alpha H\beta}$ ,  ${}^2J_{C\alpha H\beta 3}$ ,  ${}^2J_{C\beta H\alpha}$  and  ${}^3J_{H\alpha H\beta}$  splittings can help to suppress systematic discrepancies in the measurements of the much larger  ${}^1J_{C\alpha H\alpha}$ ,  ${}^1J_{C\beta H\beta 2}$ ,  ${}^1J_{C\beta H\beta 3}$  and  ${}^2J_{H\beta 2 H\beta 3}$  couplings. This effect is illustrated in Supplementary Figure 1a, and it is the reason why for a given NH or CH site, the one-bond coupling measured in the  ${}^1H$  dimension may differ from that measured in the heteronuclear dimension (Tjandra and Bax, 1997; Ding and Gronenborn, 2003). Supplementary Figure 1a shows the 2D multiplet pattern one would obtain for a CH<sub>2</sub>-TROSY experiment (using phase settings for the selection of components *a* and *h*, given in Table 1 of Miclet et al, 2004), for a C<sup>β</sup>H<sub>2</sub> site. Typically,  ${}^3J_{H\alpha H\beta 2}$  is unresolved, but as can be seen in Supplementary Figure 1a, the corresponding doublet components have unequal intensities due to intrinsically different transverse relaxation rates. This results from dipole-dipole cross-correlated relaxation between the H<sup>α</sup>-H<sup>β2</sup> and H<sup>β2</sup>-H<sup>β3</sup> interactions, denoted as  $\Gamma_{H^{\beta 2}H^{\beta 3}, H^{\beta 2}H^{\alpha}}^{DD,DD}$  (Kumar et al., 2000). The centers of the two TROSY multiplets in Supplementary Figure 1a are displaced in the  ${}^1H$  dimension by  ${}^1J_{C\beta H\beta 2} - {}^2J_{H\beta 2 H\beta 3}$  (Miclet et al., 2004), but simple peak picking will result in a smaller value. As shown in Supplementary Figure 1b, the cross correlation rate  $\Gamma_{H^{\beta 2}H^{\beta 3}, H^{\beta 2}H^{\alpha}}^{DD,DD}$  depends on the  $\chi_1$  torsion angle and can be either positive or negative with relatively large values. For example, for  $\chi_1 = 120^\circ$ ,  $\Gamma_{H^{\beta 2}H^{\beta 3}, H^{\beta 2}H^{\alpha}}^{DD,DD} = -12$  Hz for a protein with  $\tau_c S^2 = 6.7$  ns, compared to dipole-dipole auto-relaxation rates of 30 Hz for H<sup>β2</sup>H<sup>β3</sup>, and 29 Hz for C<sup>β</sup>H<sup>β2</sup>. This same large negative value is reached by  $\Gamma_{H^{\beta 3}H^{\beta 2}, H^{\beta 3}H^{\alpha}}^{DD,DD}$  for  $\chi_1 = 0^\circ$ . In weakly aligned samples,  ${}^3J_{H\alpha H\beta} + {}^3D_{H\alpha H\beta}$  may be positive or negative and the value for  ${}^1J_{C\beta H\beta 2} - {}^2J_{H\beta 2 H\beta 3} + {}^1D_{C\beta H\beta 2} - {}^2D_{H\beta 2 H\beta 3}$  measured by simple peak picking from a spectrum such as that shown in Supplementary Figure 1a can result in values that are either too large or too small. Comparison of the data recorded here, using the pulse scheme of Fig. 1b (main text), with previously reported data for  ${}^2D_{H5'H5''}$  (Miclet et al., 2003) that were

subject to the above mentioned cross-correlation problem, indicates such effects to be modest, however (pairwise rmsd 2.2 Hz,  $R_p = 0.97$ ).

The CH2-S<sup>3</sup>CT 3D experiments of Figure 1, main text, largely prevent systematic errors of the type discussed above by separating the unresolved components of the doublets of Supplementary Figure 1a into pairs of correlations (I,II) and (III,IV) that are each well separated in the <sup>13</sup>C dimension by  $^1J_{C\alpha H\alpha}$ . Similar cross-correlation terms for interactions to remote protons coupled to H<sup>β2</sup> can remain present in the measurement of  $^1J_{C\beta H\beta 2} - ^2J_{H\beta 2 H\beta 3}$ , but typically are smaller than  $\Gamma_{H^{\beta 2} H^{\beta 3}, H^{\beta 2} H^{\alpha}}^{DD, DD}$ . Analogous to the measurement of  $^1J_{C\beta H\beta 2} - ^2J_{H\beta 2 H\beta 3}$ , a small improvement in accuracy is expected for the measurement of  $^1J_{C\alpha H\alpha}$  and  $^1J_{C\beta H\beta 2} + ^1J_{C\beta H\beta 3}$  from the CH2-S<sup>3</sup>CT 3D experiments, although cross-correlated relaxation rates which could distort such measurements in the conventional <sup>1</sup>H-coupled HBCBCA experiment are much lower in the <sup>13</sup>C dimensions.

**Pulse imperfections:** Imperfect selection of single transitions can also result in systematic errors in the couplings measured from the CH2-S<sup>3</sup>CT 3D spectrum. Since no <sup>1</sup>H pulse is used between <sup>13</sup>C<sup>α</sup> and <sup>13</sup>C<sup>β</sup> labeling periods, pulse imperfections do not affect this coherence transfer process, and any magnetization transferred from <sup>13</sup>C<sup>α</sup> to <sup>13</sup>C<sup>β</sup> is subject to identical <sup>1</sup>H spin states. <sup>13</sup>C<sup>α</sup> or <sup>13</sup>C<sup>β</sup> spins for which <sup>1</sup>H<sup>α</sup> or <sup>1</sup>H<sup>β</sup> changes spin states during evolution will be largely invisible because their phase in the transverse plane is randomized by the precise moment at which the <sup>1</sup>H changes its spin state during  $t_1$  or  $t_2$ . Therefore, the accuracy of the couplings determined in the <sup>13</sup>C dimensions, *i.e.*  $^1J_{C\alpha H\alpha}$ ,  $^2J_{C\alpha H\beta 2} + ^2J_{C\alpha H\beta 3}$ ,  $^2J_{C\beta H\alpha}$  and  $^1J_{C\beta H\beta 2} + ^1J_{C\beta H\beta 3}$ , is limited primarily by the precision of the measurements.

Although spin-state-selective transfer from a given  $C_{pq}^{\beta}$  single transition ( $p$  and  $q$  corresponding to the spin states of <sup>1</sup>H<sup>β2</sup> and <sup>1</sup>H<sup>β3</sup>, respectively) to a <sup>1</sup>H single transition is achieved by the CH2-S<sup>3</sup>CT element, selectivity of such transfer is subject to <sup>1</sup>H pulse widths and transverse relaxation. Both experimental and computational evaluation of missetting the <sup>1</sup>H pulse widths during the CH2-S<sup>3</sup>CT element indicates this can have relatively severe effects, up to 7% for a <sup>1</sup>H or <sup>13</sup>C pulse error of 5% (Miclet et al., 2004). Similarly, RF inhomogeneity can adversely affect selectivity of the transfer process. Empirically we find that unwanted transfers in small molecules, where relaxation effects are negligible, are less than 2% of the selected transitions, provided <sup>1</sup>H pulse widths are

carefully calibrated and the volume of the sample is restricted to fall within the  $^1\text{H}$  receiver coil. The latter is accomplished by using a 280- $\mu\text{L}$  volume in a thin-wall Shigemi microcell (13.5 mm sample height).

**Mismatching of delays:** Effects of  $^1\text{J}_{\text{CH}}$  mismatching (Meissner et al., 1998) might be expected to be relatively large in weakly aligned samples, where the  $\tau_1 = 0.34/^1\text{J}_{\text{C}\beta\text{H}\beta}$  and  $\tau_2 = 0.23/^1\text{J}_{\text{C}\beta\text{H}\beta}$  requirements cannot be simultaneously satisfied for all methylene groups. However, numerical calculations show that the  $\text{CH}_2\text{-S}^3\text{CT}$  transfer is not very sensitive to this type of mismatching: When  $^1\text{J}_{\text{C}\beta\text{H}\beta_2}$  and  $^1\text{J}_{\text{C}\beta\text{H}\beta_3}$  are independently moved away from the ideal isotropic value by up to 30%, less than 5% of the magnetization is transferred to an unwanted transition (Supplementary Figures 2 and 3). Moreover, it is noteworthy that the corresponding artifact does not disturb the coupling measurements in the  $^1\text{H}$  dimension since it is separated by the large  $^1\text{J}_{\text{C}\beta\text{H}\beta_2} - ^2\text{J}_{\text{H}\beta_2\text{H}\beta_3}$  coupling and therefore does not cause a frequency displacement of the selected transition.

**Relaxation of passive spins:** The main source of systematic error when measuring couplings in the directly detected dimension stems from the finite life time of the spin state of the passive spin, which affects nearly all measurements of  $^1\text{H}\text{-}^1\text{H}$  couplings (Harbison, 1993). For example, a spin-flip of  $^1\text{H}^\alpha$  during data acquisition switches the  $^1\text{H}$  frequencies of transitions I and II in Figure 2 (main text), and thereby decreases their apparent splitting to less than the true value,  $^3\text{J}_{\text{H}\alpha\text{H}\beta_2}$ . In the slow tumbling limit, the  $^1\text{H}$  spin flip rate increases linearly with  $\tau_c$ , and therefore increases the underestimate of the true magnitude of the  $^1\text{H}\text{-}^1\text{H}$  coupling.

A second, analogous decrease in the  $^1\text{H}\text{-}^1\text{H}$  coupling can result from transverse relaxation of the passive spin during the  $\text{CH}_2\text{-S}^3\text{CT}$  process. In particular, the  $\text{S}^3\text{CT}$  scheme relies on the fact that the  $^1\text{H}^\alpha$  spin before and after the  $\text{CH}_2\text{-S}^3\text{CT}$  element remains unchanged. However, transverse relaxation of  $^1\text{H}^\alpha$  during this element makes this process imperfect. For a transverse relaxation time,  $T_2$ , only a fraction  $\exp[-(\tau_1 + \tau_2)/T_2]$  of  $^1\text{H}^\alpha$  z-magnetization is preserved, corresponding to a change in spin state for a fraction  $0.5(1 - \exp[-(\tau_1 + \tau_2)/T_2])$  of the  $^1\text{H}^\alpha$  spins. Similar to the above mentioned effect of flips of the  $^1\text{H}^\alpha$  spin state during data acquisition, transverse relaxation of  $^1\text{H}^\alpha$  magnetization during the  $\text{CH}_2\text{-S}^3\text{CT}$  module decreases the apparent value of the  $^3\text{J}_{\text{H}\alpha\text{H}\beta}$  coupling (see Supplementary Figure 4 for a numerical evaluation of the error). Analogously, when considering the effect of evolution due to  $^3\text{J}_{\text{H}\beta\text{H}\alpha}$  coupling during the  $\tau_1$  and  $\tau_2$  delays, not all  $^1\text{H}^\alpha$  spins are returned to their original spin state, similarly decreasing the apparent  $^3\text{J}_{\text{H}\alpha\text{H}\beta}$  coupling. However, numerical calculations and simulations (Nicholas et al., 2000)

show that this latter effect is very small, even when considering large ( ${}^3J_{\text{H}\alpha\text{H}\beta}+{}^3D_{\text{H}\alpha\text{H}\beta}$ ) couplings. For example, for  ${}^3J_{\text{H}\alpha\text{H}\beta} = 15$  Hz, less than 1% of the  $\text{H}^\alpha$  spin state is inverted during the  $\tau_1+\tau_2$  delay of the CH2-S3CT transfer, leading to errors considerably smaller (typically  $<0.1$  Hz) than those mentioned above resulting from transverse  ${}^1\text{H}^\alpha$  relaxation during  $\tau_1+\tau_2$ .

### Equations used for calculation of transverse relaxation rates.

Taking into account the following six cross-correlated relaxation rates,

$\Gamma_{H^{\beta 2}, H^{\beta 2} C^{\beta}}^{-CSA, DD}$ ,  $\Gamma_{H^{\beta 2}, H^{\beta 2} H^{\beta 3}}^{-CSA, DD}$ ,  $\Gamma_{H^{\beta 2} C^{\beta}, H^{\beta 2} H^{\beta 3}}^{-DD, DD}$ ,  $\Gamma_{C^{\beta}, C^{\beta} H^{\beta 2}}^{-CSA, DD}$ ,  $\Gamma_{C^{\beta}, C^{\beta} H^{\beta 3}}^{-CSA, DD}$  and  $\Gamma_{C^{\beta} H^{\beta 2}, C^{\beta} H^{\beta 3}}^{-DD, DD}$ , the relaxation properties of cross peaks I, II, III and IV (referring to Figure 2, main text) of the spin-state-selective experiment are given by (Miclet et al., 2004):

- In the  $^1H$  dimension ( $F_3$ ), with  $\mathfrak{R}_H$  being the  $^1H^{\beta}$  autorelaxation rate:

$$R_H^I = R_H^{II} = \mathfrak{R}_H + \Gamma_{H^{\beta 2}, H^{\beta 2} C^{\beta}}^{-CSA, DD} - \Gamma_{H^{\beta 2}, H^{\beta 2} H^{\beta 3}}^{-CSA, DD} - \Gamma_{H^{\beta 2} C^{\beta}, H^{\beta 2} H^{\beta 3}}^{-DD, DD}$$

$$R_H^{III} = R_H^{IV} = \mathfrak{R}_H - \Gamma_{H^{\beta 2}, H^{\beta 2} C^{\beta}}^{-CSA, DD} + \Gamma_{H^{\beta 2}, H^{\beta 2} H^{\beta 3}}^{-CSA, DD} - \Gamma_{H^{\beta 2} C^{\beta}, H^{\beta 2} H^{\beta 3}}^{-DD, DD}$$

- In the  $^{13}C$  dimension ( $F_2$ ), with  $\mathfrak{R}_C$  being the  $^{13}C^{\beta}$  autorelaxation rate.

$$R_C^I = R_C^{II} = \mathfrak{R}_C - \Gamma_{C^{\beta}, C^{\beta} H^{\beta 2}}^{-CSA, DD} - \Gamma_{C^{\beta}, C^{\beta} H^{\beta 3}}^{-CSA, DD} + \Gamma_{C^{\beta} H^{\beta 2}, C^{\beta} H^{\beta 3}}^{-DD, DD}$$

$$R_C^{III} = R_C^{IV} = \mathfrak{R}_C + \Gamma_{C^{\beta}, C^{\beta} H^{\beta 2}}^{-CSA, DD} + \Gamma_{C^{\beta}, C^{\beta} H^{\beta 3}}^{-CSA, DD} + \Gamma_{C^{\beta} H^{\beta 2}, C^{\beta} H^{\beta 3}}^{-DD, DD}$$

The  $^1H^{\alpha}$ -coupled HBCBCA experiment is used as a reference for the  $^1J_{C\alpha H\alpha}$  measurement in  $^{13}C$  dimension ( $F_1$ ). The relaxation properties of its components in  $F_3$  and  $F_2$  dimensions are, respectively:

$$R_H^{\text{decoupled}} = \mathfrak{R}_H$$

$$R_C^{\text{up}} = R_C^{\text{down}} = \mathfrak{R}_C + \Gamma_{C^{\beta} H^{\beta 2}, C^{\beta} H^{\beta 3}}^{-DD, DD}$$

The  $^1H^{\beta}$ -coupled HBCBCA experiment is used for comparisons of the  $^1J_{C^{\beta} H^{\beta 2}} + ^1J_{C^{\beta} H^{\beta 3}}$  measurement in the  $^{13}C$  dimension ( $F_2$ ). The relaxation properties of its components in  $F_3$  and  $F_2$  dimensions are respectively:

$$R_H^{\text{decoupled}} = \mathfrak{R}_H$$

$$R_C^{\text{up}} = \mathfrak{R}_C - \Gamma_{C^{\beta}, C^{\beta} H^{\beta 2}}^{-CSA, DD} - \Gamma_{C^{\beta}, C^{\beta} H^{\beta 3}}^{-CSA, DD} + \Gamma_{C^{\beta} H^{\beta 2}, C^{\beta} H^{\beta 3}}^{-DD, DD}$$

$$R_C^{\text{down}} = \mathfrak{R}_C + \Gamma_{C^{\beta}, C^{\beta} H^{\beta 2}}^{-CSA, DD} + \Gamma_{C^{\beta}, C^{\beta} H^{\beta 3}}^{-CSA, DD} + \Gamma_{C^{\beta} H^{\beta 2}, C^{\beta} H^{\beta 3}}^{-DD, DD}$$

### Numerical values for calculated individual auto and cross-relaxation rates.

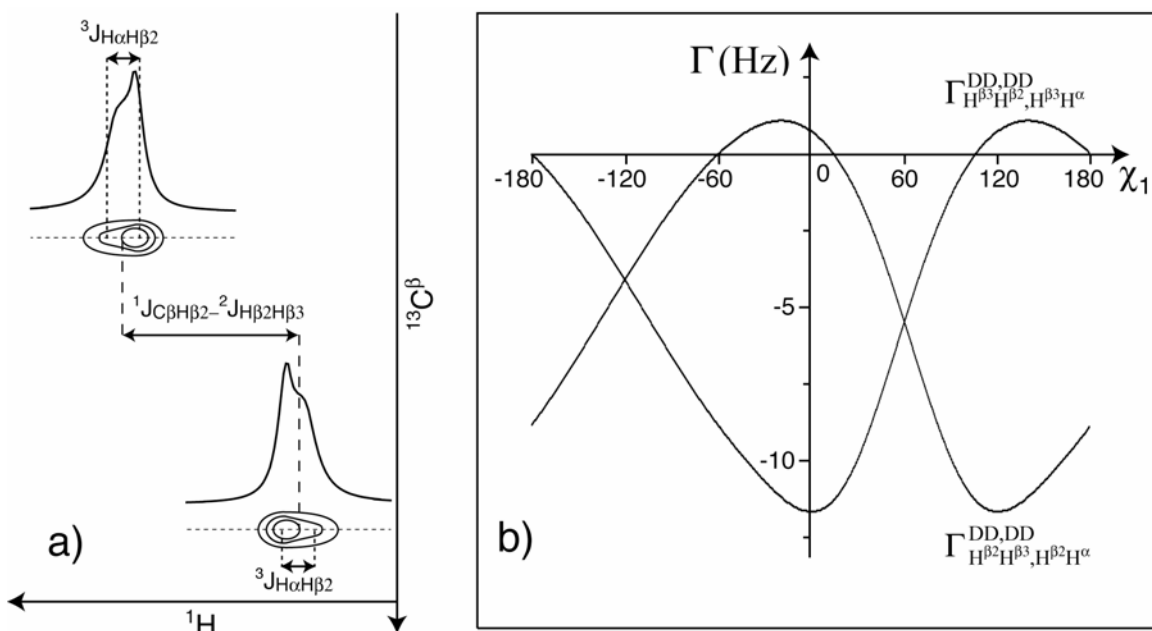
The  $^1\text{H}^\beta$  and  $^{13}\text{C}^\beta$  rates are calculated for each component of the spin-state selective 3D experiment and of the reference experiments, using  $\tau_C S^2 = 6.74$  ns and the values previously reported for the Gly methylene  $^{13}\text{C}$  CSA (Yao and Hong, 2002) and  $^1\text{H}$  CSA (Miclet et al., 2004). The calculated value for the six different cross-correlated relaxation rates involved are  $\Gamma_{\text{H}^\beta 2, \text{H}^\beta 2 \text{C}^\beta}^{\text{CSA, DD}} = 6.6$  Hz,  $\Gamma_{\text{H}^\beta 2, \text{H}^\beta 2 \text{H}^\beta 3}^{\text{CSA, DD}} = -0.2$  Hz,  $\Gamma_{\text{H}^\beta 2 \text{C}^\beta, \text{H}^\beta 2 \text{H}^\beta 3}^{\text{DD, DD}} = 27.4$  Hz,  $\Gamma_{\text{C}^\beta, \text{C}^\beta \text{H}^\beta 2}^{\text{CSA, DD}} + \Gamma_{\text{C}^\beta, \text{C}^\beta \text{H}^\beta 3}^{\text{CSA, DD}} = -13.6$  Hz,  $\Gamma_{\text{C}^\beta \text{H}^\beta 2, \text{C}^\beta \text{H}^\beta 3}^{\text{DD, DD}} = -20.5$  Hz. For a  $\text{C}^\beta$  methylene group with an  $\text{H}^\alpha$  at a distance of  $2.1\text{\AA}$  and an additional remote proton at  $2.5\text{\AA}$ , the effective transverse auto-relaxation rates are then:  $\mathfrak{R}_\text{H} = 80$  Hz,  $\mathfrak{R}_\text{C} = 66$  Hz.

Values of relaxation rates of the relevant transitions in the spin-state-selective HBCBCA and  $^1\text{H}^\beta$ -coupled and  $^1\text{H}^\alpha$ -coupled regular HBCBCA experiments, calculated from the above contributions are summarized in Table S1.

**Table S1.** Calculated transverse relaxation rates effective during  $^1\text{H}^\beta$  ( $t_3$ ) and  $^{13}\text{C}^\beta$  ( $t_2$ ) evolution for the four components of the spin-state-selective 3D experiment and for the upfield and downfield  $^{13}\text{C}$  components of  $^1\text{H}^\alpha$ -coupled and  $^1\text{H}^\beta$ -coupled reference experiments.

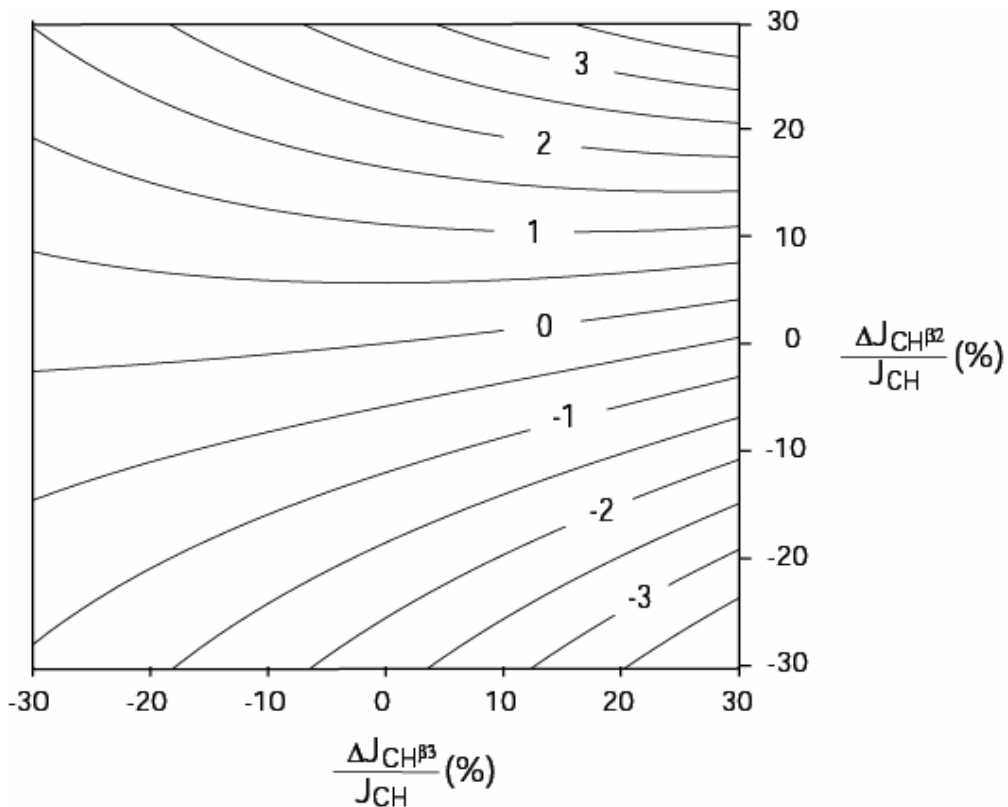
3D experiment component	spin-state selective		$\text{H}^\alpha$ -coupled HBCBCA		$\text{H}^\beta$ -coupled HBCBCA	
	I, II*	III, IV*	up	down	up	down
$R_\text{H}$ (Hz)	59.4	45.8	80	80	80	80
$R_\text{C}$ (Hz)	59.1	31.9	45.5	45.5	59.1	31.9

\* Multiplet components correspond to the correlations marked in Figure 2 of the main text.

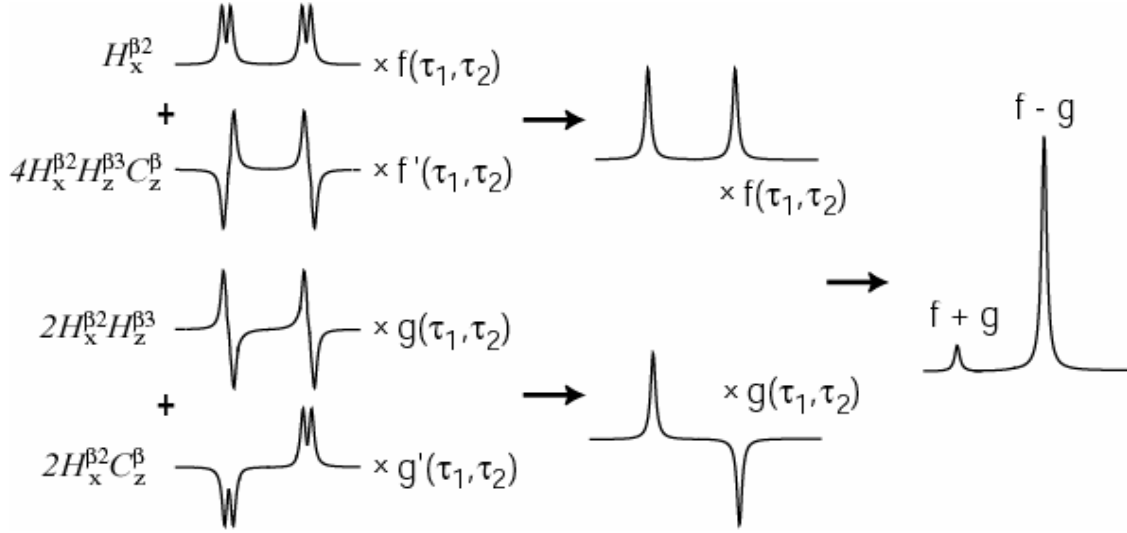


**Supplementary Figure 1.** Effect of cross-correlated relaxation on the measurement of  ${}^1J_{C\beta H\beta 2}-{}^2J_{H\beta 2 H\beta 3}$ . (a) Two-dimensional E.COSY pattern of a  $C^\beta H^\beta H^\beta$  spin system, resulting from a 2D CH<sub>2</sub>-TROSY experiment (Miclet et al., 2004). Frequency displacements correspond to  ${}^1J_{C\beta H\beta 2}+{}^1J_{C\beta H\beta 3}$  in the  $C^\beta$  dimension and to  ${}^1J_{C\beta H\beta 2}-{}^2J_{H\beta 2 H\beta 3}$  in the  $H^\beta$  dimension. Each E.COSY multiplet component consists of two unresolved components, separated by  ${}^3J_{H\beta 2 H\alpha}$ . Depending on the magnitude of the cross-correlated relaxation rate  $\Gamma_{H^{\beta 2}H^{\beta 3},H^{\beta 2}H^\alpha}^{DD,DD}$ , these two components exhibit different intensities which can affect the accuracy of the  ${}^1J_{C\beta H\beta 2}-{}^2J_{H\beta 2 H\beta 3}$  measurement. (b) Calculated cross-correlated relaxation rates  $\Gamma_{H^{\beta 2}H^{\beta 3},H^{\beta 2}H^\alpha}^{DD,DD}$ , and  $\Gamma_{H^{\beta 3}H^{\beta 2},H^{\beta 3}H^\alpha}^{DD,DD}$  as a function of  $\chi_1$ , for a protein characterized by  $\tau_c S^2 = 6.74$  ns. Significant negative values are found for the common side chain conformers:  $\Gamma_{H^{\beta 3}H^{\beta 2},H^{\beta 3}H^\alpha}^{DD,DD} = \Gamma_{H^{\beta 2}H^{\beta 3},H^{\beta 2}H^\alpha}^{DD,DD} = -5.5$  Hz for  $\chi_1 = 60^\circ$ ,  $\Gamma_{H^{\beta 2}H^{\beta 3},H^{\beta 2}H^\alpha}^{DD,DD} = -8.5$  Hz for  $\chi_1 = 180^\circ$ , and  $\Gamma_{H^{\beta 3}H^{\beta 2},H^{\beta 3}H^\alpha}^{DD,DD} = -8.5$  Hz for  $\chi_1 = -60^\circ$ . The corresponding autorelaxation rates are:  $\Gamma_{H^{\beta 2}H^{\beta 3},H^{\beta 2}H^{\beta 3}}^{DD,DD} = 30$  Hz and  $\Gamma_{C^\beta H^{\beta 2},C^\beta H^{\beta 2}}^{DD,DD} = \Gamma_{C^\beta H^{\beta 3},C^\beta H^{\beta 3}}^{DD,DD} = 29$  Hz.





**Supplementary Figure 2.** Intensity of non-selected component (%) relative to the component selected by the S<sup>3</sup>CT pulse sequence element as a function of J-mismatching. The selection of a single transition is realized when  $f(\tau_1, \tau_2) = \pm g(\tau_1, \tau_2)$  (see the legend of Figure S3 for the function definitions). Delays  $\tau_1$  and  $\tau_2$  are chosen to satisfy this equality. However, as  $f(\tau_1, \tau_2)$  and  $g(\tau_1, \tau_2)$  depend on the values of  $^1J_{C\beta H\beta 2}$  and  $^1J_{C\beta H\beta 3}$ , variation of these couplings may lead to incomplete selection. Calculations are presented to quantify the selection artifact, corresponding to the ratio  $(f-g)/(f+g)$ , as a function of  $^1J_{C\beta H\beta 2}$  and  $^1J_{C\beta H\beta 3}$  mismatch. As shown by the values reported on the graph (%), an artifact of only 4% is obtained when the  $^1J_{C\beta H\beta 2}$  and  $^1J_{C\beta H\beta 3}$  mis-matching is as high as 30 %.



**Supplementary Figure 3.** The CH<sub>2</sub>-S<sup>3</sup>CT element transfers different amount of magnetization to the four Cartesian operators  $H_x^{\beta_2}$ ,  $4H_x^{\beta_2}H_z^{\beta_3}C_z^{\beta_2}$ ,  $2H_x^{\beta_2}H_z^{\beta_3}$  and  $2H_x^{\beta_2}C_z^{\beta_2}$  as described by functions  $f(\tau_1, \tau_2)$ ,  $f'(\tau_1, \tau_2)$ ,  $g(\tau_1, \tau_2)$  and  $g'(\tau_1, \tau_2)$  (Miclet et al., 2004):

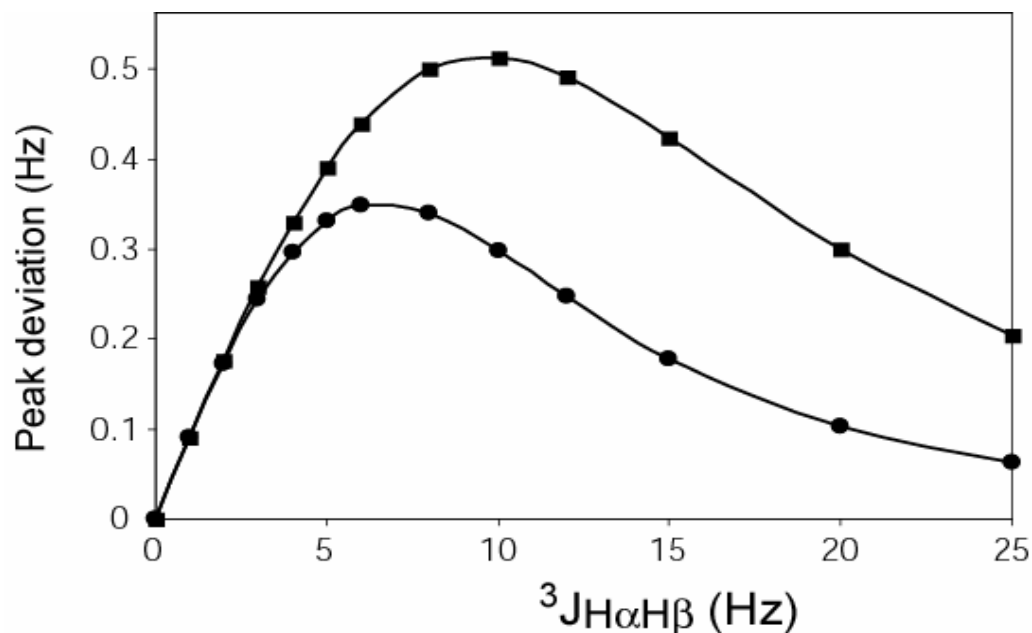
$$f(\tau_1, \tau_2) = \cos(\pi {}^1J_{C\beta H\beta_3} \tau_1) \sin(\pi {}^1J_{C\beta H\beta_2} \tau_2) + \sin(\pi {}^1J_{C\beta H\beta_2} \tau_1)$$

$$f'(\tau_1, \tau_2) = -\cos(\pi {}^1J_{C\beta H\beta_3} \tau_1) \sin(\pi {}^1J_{C\beta H\beta_2} \tau_2) - \sin(\pi {}^1J_{C\beta H\beta_2} \tau_1)$$

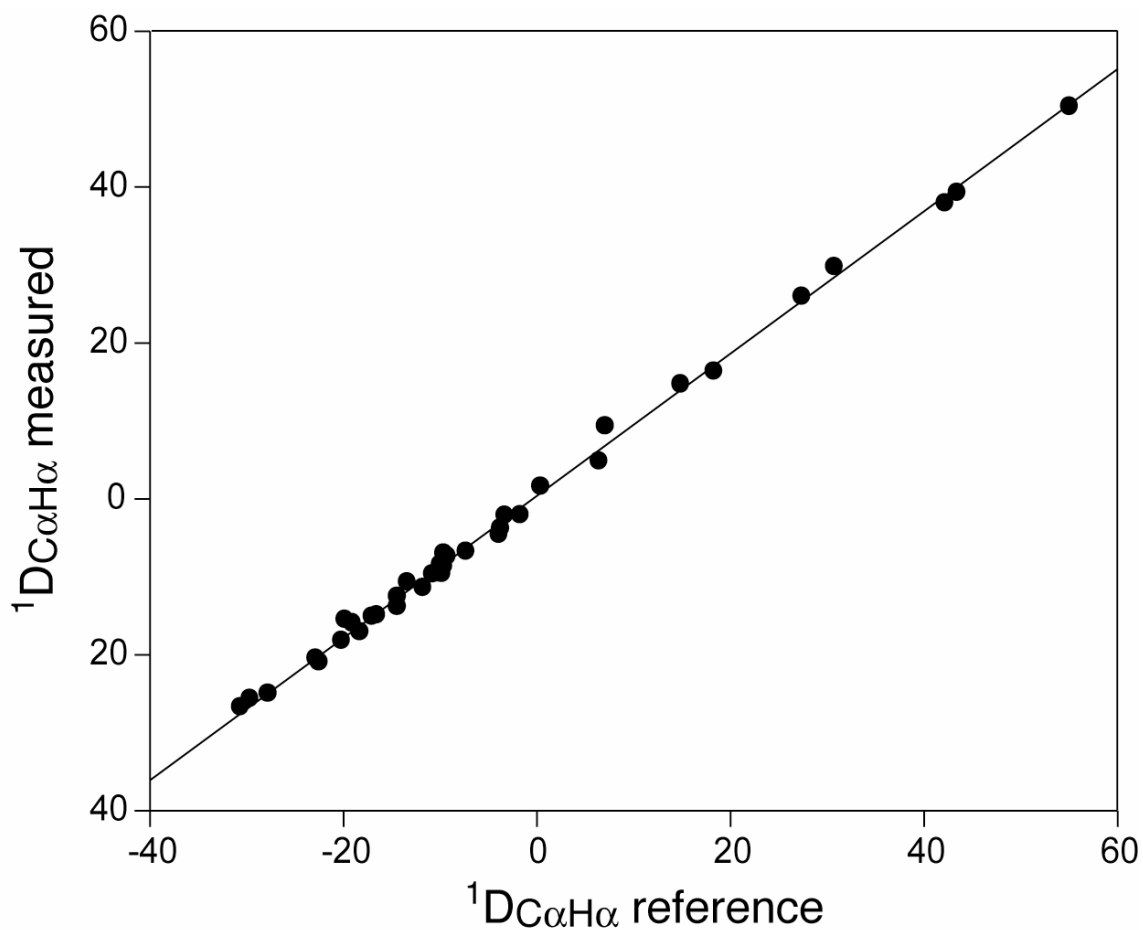
$$g(\tau_1, \tau_2) = \sin(\pi {}^1J_{C\beta H\beta_2} \tau_1) \cos(\pi {}^1J_{C\beta H\beta_3} \tau_1) \cos(\pi {}^1J_{C\beta H\beta_3} \tau_2) + \sin(\pi {}^1J_{C\beta H\beta_2} \tau_2) \cos(\pi {}^1J_{C\beta H\beta_3} \tau_2) \\ + \sin(\pi {}^1J_{C\beta H\beta_2} \tau_1) \sin(\pi {}^1J_{C\beta H\beta_3} \tau_1) \cos(\pi {}^1J_{C\beta H\beta_2} \tau_2) \sin(\pi {}^1J_{C\beta H\beta_3} \tau_2)$$

$$g'(\tau_1, \tau_2) = -\sin(\pi {}^1J_{C\beta H\beta_2} \tau_1) \cos(\pi {}^1J_{C\beta H\beta_3} \tau_1) \cos(\pi {}^1J_{C\beta H\beta_3} \tau_2) - \sin(\pi {}^1J_{C\beta H\beta_2} \tau_2) \cos(\pi {}^1J_{C\beta H\beta_3} \tau_2) \\ - \sin(\pi {}^1J_{C\beta H\beta_2} \tau_1) \sin(\pi {}^1J_{C\beta H\beta_3} \tau_1) \cos(\pi {}^1J_{C\beta H\beta_2} \tau_2) \sin(\pi {}^1J_{C\beta H\beta_3} \tau_2)$$

Since  $f(\tau_1, \tau_2) = -f'(\tau_1, \tau_2)$ , and  $g(\tau_1, \tau_2) = -g'(\tau_1, \tau_2)$ , transitions  $H_{++}^{\beta_2} = 1/4 (H_x^{\beta_2} + 4H_x^{\beta_2}H_z^{\beta_3}C_z^{\beta_2} + 2H_x^{\beta_2}H_z^{\beta_3} + 2H_x^{\beta_2}C_z^{\beta_2})$  and  $H_{--}^{\beta_2} = 1/4 (H_x^{\beta_2} + 4H_x^{\beta_2}H_z^{\beta_3}C_z^{\beta_2} - 2H_x^{\beta_2}H_z^{\beta_3} - 2H_x^{\beta_2}C_z^{\beta_2})$ , cancel ( $H_{pq}^{\beta_2}$  refers to a single transition where  $p$  and  $q$  denote the spin states of  $^{13}C^{\beta_2}$  and  $^1H^{\beta_3}$ , respectively). The two remaining, observable transitions  $H_{+-}^{\beta_2}$  and  $H_{-+}^{\beta_2}$  are separated by  ${}^1J_{C\beta H\beta_2} - 2J_{H\beta_2 H\beta_3}$ .



**Supplementary Figure 4.** Error in peak position in the  $F_3$  ( $^1H$ ) dimension resulting from  $^1H^\alpha$  transverse relaxation during the  $S^3CT$  element, as a function of the true value of the  $^3J_{H\alpha H\beta}$  coupling, assuming a  $^1H^\alpha$   $T_2$  value of 20 ms. For this case, calculations predict 10% of  $^1H^\alpha$  spins change their eigenstates, creating a 10% unresolved artifact, separated by  $^3J_{H\alpha H\beta}$  from the selected single transition and affecting its apparent position. Simulations (Nicholas et al., 2000) have been carried out to assess the frequency deviation resulting from this effect. Two curves have been plotted as a function of  $^3J_{H\alpha H\beta}$ , for a  $^1H$  line width of 20 Hz (●) and 30 Hz (■). A frequency displacement of up to 0.5 Hz is obtained for  $^3J_{H\alpha H\beta} = 10$  Hz and a  $^1H$  line width of 30 Hz. As this deviation equally affects both components of the doublet, but in opposite directions, the coupling can be underestimated by up to 1 Hz.



**Supplementary Figure 5.** Comparison of 38  $^1D_{C\alpha H\alpha}$  dipolar couplings, measured for non-overlapping correlations in a regular 800 MHz  $^1H$ -coupled  $^1H$ - $^{13}C$  HSQC of GB3, with values previously reported for GB3 in Pf1. The solid line corresponds to a scaling factor of 0.93. The correlation coefficient between the earlier and new measurement is  $R_p = 0.998$ .

**Tables of measured couplings. (Tables A, B, C, D, E, F)**

Tables A and B correspond to the couplings measured for protein GB3, in isotropic solution and in a medium containing 10 mg/ml liquid crystalline Pf1, respectively.

Tables C and D correspond to the couplings measured for the RNA oligomer, in an isotropic phase and in a solution containing 20 mg/ml liquid crystalline Pf1, respectively.

For each measurement, the error  $\Delta$ , corresponds to:

$$\sqrt{\frac{(\Delta v_1)^2 + (\Delta v_2)^2}{2 \times (S/N)^2}}, \text{ where } \Delta v_1 \text{ and } \Delta v_2 \text{ are the line width of the two peaks used for the}$$

coupling determination and S/N is the signal to noise ratio. Then, for the same coupling, an average value is obtained by weighing all the available splitting values by the squared inverse of their experimental uncertainty. The error in the average is calculated as the propagated error of the individual measurements. Entries “ov” refer to peaks partially overlapping and for which the coupling determination may be inaccurate; “\*” indicates that no measurement was possible, due to extensive overlap. Tables E and F correspond to the residual dipolar couplings obtained for GB3 and for the RNA oligomer, respectively.

Table A

Tab. A	ЖСН <sub>н</sub>	Δ	ЖСН <sub>н2</sub> + ЖСН <sub>н3</sub>	Δ	ЖСН <sub>н2</sub> + ЖСН <sub>н3</sub>	Δ	ЖСН <sub>н</sub>	Δ	ЖСН <sub>н2</sub> – ЖСН <sub>н3</sub>	Δ	ЖСН <sub>н3</sub> – ЖСН <sub>н2</sub>	Δ	ЖСН <sub>н</sub>	Δ	ЖСН <sub>н</sub>	Δ	ЖСН <sub>н3</sub>	ЖСН <sub>н2</sub>	ЖСН <sub>н3</sub>
y3	144.97	0.86	-8.19	1.35	255.73	0.70	-4.02	0.50											
	145.38	1.14	-8.81	1.34	255.92	0.72	-4.30	0.66											
	145.27	2.38	-7.88	2.26	256.12	1.36	-3.63	1.44	141.45	0.73	141.18	0.77	1.86	0.50	12.04	0.80			
	146.35	1.89	-7.85	1.89	255.35	1.10	-4.87	1.13	140.58	1.36	141.90	1.20	2.74	1.46	11.32	1.18			
	<b>145.26</b>	0.62	<b>-8.31</b>	0.80	<b>255.78</b>	0.43	<b>-4.17</b>	0.36	<b>141.26</b>	0.65	<b>141.39</b>	0.65	<b>1.95</b>	0.48	<b>11.81</b>	0.66	-13.43	127.82	127.96
n8	140.49	0.18	-10.91	0.22	260.74	0.11	-4.74	0.10											
	140.43	0.18	-10.97	0.22	260.67	0.1	-4.82	0.10											
	140.49	0.26	-10.91	0.25	260.40	0.14	-5.09	0.15	146.11	0.10	145.78	0.10	7.15	0.09	6.00	0.09			
	140.45	0.26	-10.95	0.25	260.56	0.14	-4.93	0.14	146.34	0.12	145.52	0.13	6.92	0.13	6.26	0.13			
	<b>140.46</b>	0.10	<b>-10.94</b>	0.12	<b>260.63</b>	0.06	<b>-4.86</b>	0.06	<b>146.20</b>	0.08	<b>145.68</b>	0.08	<b>7.07</b>	0.07	<b>6.09</b>	0.08	-15.63	130.57	130.06
d22	139.97	0.44	-6.76	2.51	260.71	1.18	-3.56	0.24											
	140.21	0.57	-7.23	1.20	260.67	0.56	-3.98	0.30											
	140.03	2.13	-6.70	0.59	260.75	0.33	-3.52	1.20	149.02	0.63	143.45	1.15	4.02	0.32	2.12	0.21			
	140.43	1.04	-7.01	0.62	260.91	0.34	-3.74	0.58	149.16	0.36	143.18	0.30	3.87	0.65	2.39	1.17			
	<b>140.10</b>	0.33	<b>-6.89</b>	0.40	<b>260.80</b>	0.21	<b>-3.72</b>	0.18	<b>149.12</b>	0.31	<b>143.20</b>	0.29	<b>3.99</b>	0.29	<b>2.13</b>	0.21	-15.76	133.36	127.44
f30	143.25	0.45	-8.95	1.25	258.34	0.60	-5.45	0.26											
	143.91	0.48	-9.27	1.32	258.39	0.66	-5.06	0.28											
	143.66	1.39	-8.54	1.01	258.10	0.55	-5.69	0.77	144.11	0.64	146.75	0.81	0.71	0.26	11.30	0.32			
	143.58	1.38	-9.59	0.94	257.92	0.51	-5.53	0.79	143.67	0.59	146.45	0.55	1.15	0.83	11.60	0.93			
	<b>143.56</b>	0.31	<b>-9.10</b>	0.55	<b>258.15</b>	0.29	<b>-5.30</b>	0.18	<b>143.88</b>	0.43	<b>146.55</b>	0.46	<b>0.75</b>	0.25	<b>11.33</b>	0.30	-16.14	127.74	130.41
n35	150.96	0.08	-10.14	0.19	262.08	0.09	-4.94	0.05											
	150.76	ov	-9.86	ov	261.92	ov	-4.62	ov											
	150.98	0.21	-10.11	0.16	262.15	0.09	-4.87	0.12	147.78	0.08	145.76	0.06	7.92	0.04	7.07	ov			
	150.70	0.10	-9.92	ov	261.66	ov	-4.89	0.06	147.78	0.08	145.69	0.06	7.92	0.11	7.15	0.05			
	<b>150.87</b>	0.06	<b>-10.12</b>	0.12	<b>262.12</b>	0.06	<b>-4.92</b>	0.03	<b>147.78</b>	0.06	<b>145.73</b>	0.04	<b>7.92</b>	0.04	<b>7.15</b>	0.05	-15.70	132.08	130.03
d36	149.54	0.16	-11.37	ov	255.29	ov	-5.47	0.09											
	149.38	0.19	-7.52	0.33	256.35	0.15	-5.55	0.11											
	149.36	ov	-11.56	ov	257.80	ov	-3.00	ov	144.21	0.16	150.54	ov	2.12	0.11	11.40	0.08			
	149.36	0.35	-7.54	0.28	256.52	0.16	-5.39	0.19	143.64	0.15	150.36	ov	2.69	0.19	11.59	ov			
	<b>149.47</b>	0.11	<b>-7.53</b>	0.21	<b>256.43</b>	0.11	<b>-5.49</b>	0.07	<b>143.90</b>	0.11	<b>150.45</b>	ov	<b>2.25</b>	0.09	<b>11.40</b>	0.08	-18.96	124.94	131.49
n37	140.40	0.33	-10.41	0.35	263.15	0.17	-5.42	0.19											
	140.28	0.37	-10.22	0.39	263.22	0.19	-5.58	0.21											
	140.14	0.42	-10.66	0.45	263.34	0.25	-5.23	0.24	149.03	0.17	144.24	0.18	2.04	0.19	12.13	0.19			
	139.77	0.49	-10.73	0.51	263.21	0.29	-5.60	0.28	149.32	0.25	143.84	0.27	1.76	0.24	12.52	0.26			
	<b>140.21</b>	0.20	<b>-10.46</b>	0.20	<b>263.21</b>	0.11	<b>-5.45</b>	0.11	<b>149.12</b>	0.14	<b>144.12</b>	0.15	<b>1.94</b>	0.15	<b>12.27</b>	0.15	-15.01	134.11	129.10
d40	140.81	0.14	-10.59	0.23	261.66	0.11	-4.06	0.07											
	140.83	0.16	-10.90	0.21	261.61	0.1	-3.97	0.08											
	140.85	0.28	-10.55	0.24	261.43	0.13	-4.29	0.15	147.13	0.10	145.78	0.11	10.16	0.06	3.67	0.08			
	141.31	0.24	-10.43	0.22	261.50	0.12	-4.07	0.13	147.01	0.11	145.88	0.12	10.28	0.14	3.57	0.13			
	<b>140.89</b>	0.09	<b>-10.63</b>	0.11	<b>261.56</b>	0.06	<b>-4.06</b>	0.05	<b>147.07</b>	0.08	<b>145.83</b>	0.08	<b>10.18</b>	0.06	<b>3.64</b>	0.07	-15.67	131.40	130.16
w43	145.40	0.51	-8.31	4.35	255.37	1.88	-3.98	0.28											
	145.43	0.57	-7.38	2.43	255.00	1.04	-4.11	0.32											
	147.23	5.54	-6.47	4.22	254.55	2.19	-4.79	2.88	141.61	2.43	146.34	1.20	1.79	0.32	11.20	0.34			
	145.76	2.72	-7.05	1.90	254.46	0.99	-4.65	1.40	142.36	2.29	147.63	0.97	1.03	3.33	9.91	1.50			
	<b>145.43</b>	0.37	<b>-7.21</b>	1.34	<b>254.78</b>	0.64	<b>-4.05</b>	0.21	<b>142.01</b>	1.67	<b>147.12</b>	0.75	<b>1.78</b>	0.31	<b>11.13</b>	0.33	-17.18	124.83	129.94
y45	143.18	0.57	-12.06	1.40	265.35	0.69	-3.95	0.32											
	142.72	0.60	-11.72	ov	265.31	ov	-3.73	0.34											
	143.27	2.8	-11.98	2.6	265.55	1.5	-3.75	1.62	143.22	2.28	146.67	0.78	11.18	0.40	4.35	0.39			
	140.89	ov	-13.55	ov	264.38	ov	-4.65	ov	142.76	2.04	144.96	1.84	11.65	ov	6.06	1.96			
	<b>142.97</b>	0.41	<b>-12.04</b>	1.23	<b>265.39</b>	0.63	<b>-3.84</b>	0.23	<b>142.97</b>	1.52	<b>146.41</b>	0.72	<b>11.18</b>	0.40	<b>4.41</b>	0.38	-11.99	130.97	134.41
d46	143.16	0.26	-11.81	0.70	262.33	0.33	-3.85	0.15											
	143.04	0.27	-11.41	0.64	262.17	0.3	-3.72	0.16											
	143.57	0.73	-11.40	0.50	262.23	0.3	-3.95	0.42	145.85	0.32	146.09	0.31	11.79	0.14	3.39	0.16			
	143.04	0.74	-11.41	0.57	261.72	0.34	-4.17	0.43	145.66	0.27	145.88	0.35	11.98	0.39	3.60	0.44			
	<b>143.13</b>	0.18	<b>-11.48</b>	0.29	<b>262.13</b>	0.16	<b>-3.82</b>	0.10	<b>145.74</b>	0.20	<b>146.00</b>	0.23	<b>11.81</b>	0.13	<b>3.41</b>	0.15	-14.81	130.93	131.19
d47	147.88	0.22	-10.50	0.36	264.29	0.17	-5.11	0.12											
	148.36	0.23	-10.93	0.36	264.26	0.18	-5.35	0.13											
	147.26	0.39	-11.12	0.32	263.67	0.18	-5.73	0.22	146.53	0.15	142.76	0.18	10.98	0.11	3.51	0.12			
	148.05	0.36	-11.24	0.30	264.17	0.17	-5.44	0.21	146.12	0.14	142.45	0.19	11.40	0.17	3.82	0.23			
	<b>147.99</b>	0.14	<b>-10.98</b>	0.17	<b>264.11</b>	0.09	<b>-5.32</b>	0.08	<b>146.31</b>	0.10	<b>142.61</b>	0.13	<b>11.10</b>	0.09	<b>3.58</b>	0.11	-12.41	133.90	130.20
f52	146.03	0.49	-7.76	3.03	259.95	1.42	-3.78	0.27											
	144.98	1.04	-7.94	0.76	259.61	0.37	-3.49	0.58											
	144.66	3.46	-9.14	2.41	259.34	1.44	-4.40	2.00	143.22	1.51	141.68	0.42	10.68	0.32	2.31	0.65			
	144.62	0.72	-8.30	1.07	258.99	0.61	-4.10	0.41	143.35	1.48	142.13	0.68	10.55	2.09	1.86	0.47			
	<b>145.50</b>	0.37	<b>-8.11</b>	0.59	<b>259.46</b>	0.30	<b>-3.83</b>	0.21	<b>143.29</b>	1.06	<b>141.80</b>	0.36	<b>10.68</b>	0.31	<b>2.01</b>	0.38	-12.81	130.47	128.99

Table B

Tab. B	ЈСаНх	Δ	ЈСрНв2 + ЈСаНв3	Δ	ЈСрНв2 + ЈСрНв3	Δ	ЈСрНх	Δ	ЈСрНв2 – ЈНв2Нв3	Δ	ЈСрНв3 – ЈНв2Нв3	Δ	ЈНв2Нх	Δ	ЈНв3Нх	Δ	ЈНв2Нв3	ЈСрНв2	ЈСрНв3
y3	117.92	0.50	-4.90	0.55	277.99	0.27	-6.52	0.24											
	118.26	0.85	-4.70	1.03	277.92	0.51	-6.46	0.42											
	117.21	0.68	-5.61	0.64	277.98	0.31	-6.53	0.34	178.66	0.40	112.39	0.94	6.38	0.35	6.01	0.67			
	116.83	1.28	-6.14	1.14	277.80	0.58	-6.59	0.65	178.83	0.45	112.11	0.87	6.21	0.49	6.29	1.10			
	<b>117.71</b>	<b>0.35</b>	<b>-5.23</b>	<b>0.36</b>	<b>277.96</b>	<b>0.18</b>	<b>-6.52</b>	<b>0.17</b>	<b>178.73</b>	<b>0.30</b>	<b>112.24</b>	<b>0.64</b>	<b>6.32</b>	<b>0.28</b>	<b>6.09</b>	<b>0.57</b>	-6.50	172.23	105.73
n8	127.58	0.17	-14.78	0.20	275.67	0.10	-6.96	0.08											
	127.82	0.17	-14.67	0.20	275.83	0.10	-6.98	0.08											
	128.21	0.25	-14.16	0.23	275.85	0.11	-6.78	0.12	142.30	0.10	149.85	0.10	5.77	0.08	0.56	0.08			
	127.93	0.25	-14.56	0.23	275.82	0.11	-6.99	0.12	142.13	0.11	149.63	0.11	5.94	0.12	0.77	0.13			
	<b>127.82</b>	<b>0.10</b>	<b>-14.57</b>	<b>0.11</b>	<b>275.79</b>	<b>0.05</b>	<b>-6.94</b>	<b>0.05</b>	<b>142.22</b>	<b>0.07</b>	<b>149.75</b>	<b>0.08</b>	<b>5.82</b>	<b>0.07</b>	<b>0.62</b>	<b>0.07</b>	-8.09	134.13	141.66
d22	124.57	0.33	-11.14	0.95	293.87	0.46	-6.10	0.16											
	124.85	0.38	-10.33	0.43	294.00	0.21	-5.89	0.18											
	125.42	1.11	-10.29	0.67	295.15	0.34	-4.82	0.55	138.04	0.25	110.51	0.58	-3.01	0.20	2.19	0.19			
	124.88	0.45	-10.30	0.40	294.71	0.20	-5.17	0.23	137.90	0.21	110.40	0.40	-2.87	0.26	2.31	0.68			
	<b>124.76</b>	<b>0.21</b>	<b>-10.37</b>	<b>0.26</b>	<b>294.45</b>	<b>0.13</b>	<b>-5.79</b>	<b>0.10</b>	<b>137.96</b>	<b>0.16</b>	<b>110.44</b>	<b>0.33</b>	<b>-2.96</b>	<b>0.16</b>	<b>2.20</b>	<b>0.18</b>	23.03	160.99	133.47
f30	128.69	0.67	-13.85	0.91	253.58	0.47	-8.05	0.33											
	128.79	0.72	-14.05	1.03	253.27	0.55	-8.18	0.36											
	127.83	1.15	-14.70	0.98	253.23	0.50	-8.40	0.60	171.20	0.73	142.75	0.67	-0.64	0.53	7.54	0.49			
	127.36	1.38	-15.48	1.17	252.59	0.59	-8.86	0.72	171.69	0.78	143.20	0.80	-1.13	0.93	7.09	0.92			
	<b>128.48</b>	<b>0.43</b>	<b>-14.43</b>	<b>0.50</b>	<b>253.22</b>	<b>0.26</b>	<b>-8.21</b>	<b>0.21</b>	<b>171.43</b>	<b>0.53</b>	<b>142.93</b>	<b>0.51</b>	<b>-0.76</b>	<b>0.46</b>	<b>7.44</b>	<b>0.43</b>	-30.57	140.86	112.36
n35	192.05	0.12	-13.78	0.30	284.32	0.16	-5.57	0.06											
	187.09	ov	-15.71	ov	284.82	ov	-5.23	ov											
	192.77	0.43	-13.06	0.33	284.78	0.16	-5.11	0.22	137.81	0.15	139.09	0.67	5.71	0.06	5.66	ov			
	193.42	0.13	-9.38	ov	285.08	ov	-4.97	0.07	137.79	0.16	140.25	0.67	5.74	0.21	4.50	0.06			
	<b>192.70</b>	<b>0.09</b>	<b>-13.46</b>	<b>0.22</b>	<b>284.54</b>	<b>0.11</b>	<b>-5.27</b>	<b>0.04</b>	<b>137.80</b>	<b>0.11</b>	<b>139.67</b>	<b>0.47</b>	<b>5.72</b>	<b>0.06</b>	<b>4.50</b>	<b>0.06</b>	3.53	141.33	143.20
d36	143.14	0.35	9.42	ov	229.88	ov	-0.20	0.18											
	143.28	0.39	1.56	0.57	229.53	0.28	-0.02	0.20											
	187.09	ov	34.53	ov	224.85	ov	-5.23	ov	151.48	0.34	155.07	ov	14.56	0.23	17.16	0.18			
	143.20	0.69	1.48	0.55	229.49	0.27	-0.06	0.33	151.72	0.31	166.56	ov	14.32	0.39	5.66	ov			
	<b>143.20</b>	<b>0.24</b>	<b>1.52</b>	<b>0.40</b>	<b>229.51</b>	<b>0.19</b>	<b>-0.11</b>	<b>0.12</b>	<b>151.62</b>	<b>0.23</b>	<b>ov</b>	<b>ov</b>	<b>14.50</b>	<b>0.20</b>	<b>17.16</b>	<b>0.18</b>	*	*	*
n37	115.16	0.41	-14.17	0.43	224.43	0.24	-7.66	0.22											
	115.37	0.70	-14.42	0.72	224.52	0.40	-7.42	0.39											
	114.40	0.53	-14.94	0.51	224.45	0.28	-7.64	0.29	153.94	0.23	135.02	0.54	-4.73	0.21	7.78	0.51			
	114.93	0.87	-14.86	0.86	224.38	0.47	-7.56	0.48	154.15	0.27	135.29	0.61	-4.93	0.29	7.51	0.63			
	<b>114.96</b>	<b>0.28</b>	<b>-14.52</b>	<b>0.28</b>	<b>224.44</b>	<b>0.16</b>	<b>-7.61</b>	<b>0.15</b>	<b>154.03</b>	<b>0.18</b>	<b>135.14</b>	<b>0.40</b>	<b>-4.80</b>	<b>0.17</b>	<b>7.67</b>	<b>0.40</b>	-32.36	121.67	102.77
d40	157.37	0.09	-8.26	0.15	261.90	0.07	-0.32	0.04											
	157.81	0.16	-8.17	0.18	261.91	0.08	-0.35	0.07											
	157.29	0.19	-8.34	0.15	261.87	0.07	-0.35	0.08	156.57	0.07	123.85	0.10	17.43	0.04	4.04	0.08			
	157.62	0.22	-8.36	0.20	261.88	0.09	-0.39	0.10	156.71	0.07	123.97	0.10	17.29	0.09	3.92	0.11			
	<b>157.47</b>	<b>0.07</b>	<b>-8.28</b>	<b>0.08</b>	<b>261.89</b>	<b>0.04</b>	<b>-0.34</b>	<b>0.03</b>	<b>156.64</b>	<b>0.05</b>	<b>123.91</b>	<b>0.07</b>	<b>17.41</b>	<b>0.04</b>	<b>4.00</b>	<b>0.07</b>	-9.33	147.31	114.58
w43	135.30	0.59	-7.20	1.72	296.30	0.90	-7.52	0.29											
	134.44	1.26	-7.64	1.97	295.99	1.00	-7.97	0.63											
	135.02	2.28	-7.49	1.61	296.23	0.78	-7.59	1.15	145.25	1.18	103.17	1.23	-0.90	0.37	7.15	0.88			
	135.10	2.47	-6.98	1.96	296.02	0.98	-7.94	1.25	144.71	1.19	105.12	1.19	-0.36	1.64	5.20	1.47			
	<b>135.14</b>	<b>0.51</b>	<b>-7.34</b>	<b>0.90</b>	<b>296.16</b>	<b>0.45</b>	<b>-7.61</b>	<b>0.25</b>	<b>144.98</b>	<b>0.84</b>	<b>104.17</b>	<b>0.85</b>	<b>-0.88</b>	<b>0.36</b>	<b>6.64</b>	<b>0.75</b>	23.50	168.48	127.67
y45	129.77	0.56	-18.20	0.86	236.99	0.42	-6.71	0.28											
	130.19	0.53	-17.75	0.85	236.45	0.40	-7.24	0.26											
	130.22	1.22	-17.74	1.04	236.62	0.47	-7.08	0.56	164.68	0.59	153.14	0.58	6.36	0.33	-1.41	0.33			
	129.35	1.14	-18.58	0.93	237.12	0.44	-6.57	0.53	164.41	0.57	152.52	0.69	6.63	0.75	-0.79	0.84			
	<b>129.95</b>	<b>0.35</b>	<b>-18.07</b>	<b>0.46</b>	<b>236.79</b>	<b>0.21</b>	<b>-6.96</b>	<b>0.17</b>	<b>164.54</b>	<b>0.41</b>	<b>152.88</b>	<b>0.44</b>	<b>6.40</b>	<b>0.31</b>	<b>-1.32</b>	<b>0.31</b>	-40.32	124.22	112.56
d46	138.49	0.37	-17.36	0.75	299.30	0.27	-6.55	0.17											
	138.36	0.26	-15.80	0.34	299.37	0.16	-6.42	0.12											
	140.93	0.93	-14.91	0.67	299.64	0.30	-6.22	0.36	107.00	0.40	150.12	0.18	8.46	0.23	-3.10	0.14			
	139.03	0.43	-15.13	0.37	299.67	0.17	-6.12	0.20	108.24	0.39	150.23	0.19	7.22	0.51	-3.20	0.23			
	<b>138.63</b>	<b>0.19</b>	<b>-15.60</b>	<b>0.22</b>	<b>299.49</b>	<b>0.10</b>	<b>-6.38</b>	<b>0.09</b>	<b>107.63</b>	<b>0.28</b>	<b>150.17</b>	<b>0.13</b>	<b>8.25</b>	<b>0.21</b>	<b>-3.12</b>	<b>0.12</b>	20.85	128.47	171.02
d47	126.19	0.22	-15.52	0.30	265.54	0.15	-8.83	0.12											
	126.38	0.27	-15.89	0.35	265.61	0.17	-8.67	0.14											
	126.80	0.37	-15.11	0.31	266.02	0.15	-8.35	0.18	135.21	0.17	164.84	0.16	5.93	0.13	0.20	0.11			
	126.86	0.43	-15.21	0.37	265.96	0.18	-8.32	0.21	135.47	0.18	164.76	0.16	5.68	0.21	0.28	0.20			
	<b>126.39</b>	<b>0.15</b>	<b>-15.38</b>	<b>0.16</b>	<b>265.77</b>	<b>0.08</b>	<b>-8.63</b>	<b>0.07</b>	<b>135.34</b>	<b>0.12</b>	<b>164.80</b>	<b>0.11</b>	<b>5.86</b>	<b>0.11</b>	<b>0.22</b>	<b>0.10</b>	-17.18	118.15	147.62
f52	137.27	0.83	*	ov	295.22	0.37	-6.89	0.44											
	135.58	1.21	-11.94	0.72	*	ov	-6.80	0.65											
	135.25	0.70	*	ov	295.11	0.42	-7.00	0.35	*	ov	64.07	ov	7.13	ov	-4.18	0.68			
	*	ov	-13.95	0.81	*	ov	*	ov											

Table C(1)

Tab. C	JC4'H4'	Δ	JC4'H5'+ JC4'H5''	Δ	JC5'H5'+ JC5'H5''	Δ	JC5'H4'	Δ	JC5'H5'- JH5'H5''	Δ	JC5'H5''	Δ	JH5'H4'	Δ	JH5'H4''	Δ	JH5'H5''	JC5'H5'	JC5'H5''
G38	148.61	1.45	*	ov	295.21	1.21	3.65	0.83											
	148.01	1.93	*	ov	297.83	1.47	2.85	1.19											
	*	ov	-8.78	2.71	296.36	1.39	2.50	1.65	157.50	1.14	157.14	1.35	0.83	0.77	2.43	1.05			
	152.61	1.44	-2.34	2.45	296.18	1.42	4.50	1.66	158.53	1.48	156.71	1.58	1.85	1.71	2.00	1.79			
<b>148.39</b>	<b>1.16</b>	<b>-5.24</b>	<b>1.82</b>	<b>296.27</b>	<b>0.68</b>	<b>3.42</b>	<b>0.59</b>	<b>157.89</b>	<b>0.91</b>	<b>156.96</b>	<b>1.03</b>	<b>1.00</b>	<b>0.70</b>	<b>2.32</b>	<b>0.91</b>				
G39	149.57	0.91	-3.84	1.26	297.26	0.78	2.65	0.58											
	*	ov	*	ov	297.20	0.83	2.66	0.59											
	147.16	1.71	-1.43	1.47	296.49	0.91	3.42	1.05	159.20	0.75	157.07	0.73	0.51	0.54	3.59	0.52			
	152.61	1.44	*	ov	296.27	0.92	3.58	1.09	159.00	0.90	156.62	0.94	0.31	1.04	2.14	1.07			
<b>149.03</b>	<b>0.81</b>	<b>-2.82</b>	<b>0.96</b>	<b>296.86</b>	<b>0.43</b>	<b>2.85</b>	<b>0.36</b>	<b>159.12</b>	<b>0.58</b>	<b>156.52</b>	<b>0.57</b>	<b>0.47</b>	<b>0.48</b>	<b>3.31</b>	<b>0.47</b>				
C40	148.86	0.90	-2.25	1.21	297.49	0.71	0.54	2.16											
	150.05	0.77	-5.80	1.06	297.79	0.62	0.46	1.84											
	151.83	1.77	-5.23	1.57	297.39	0.95	1.06	4.23	159.96	0.68	156.53	0.54	1.73	0.51	1.73	0.39			
	152.61	1.44	-8.36	1.25	296.21	0.74	0.85	3.40	160.27	0.88	156.17	0.67	2.05	0.98	1.37	0.77			
<b>150.14</b>	<b>0.52</b>	<b>-5.41</b>	<b>0.62</b>	<b>297.27</b>	<b>0.37</b>	<b>0.59</b>	<b>1.24</b>	<b>160.08</b>	<b>0.54</b>	<b>156.39</b>	<b>0.42</b>	<b>1.80</b>	<b>0.46</b>	<b>1.65</b>	<b>0.35</b>				
U41	147.07	0.85	-1.38	1.20	298.67	0.75	3.22	0.51											
	*	ov	*	ov	297.90	0.49	3.33	0.36											
	151.54	1.72	-5.85	1.50	298.11	0.98	3.78	1.12	161.53	0.65	156.17	0.43	3.17	0.46	2.18	0.31			
	152.61	1.44	*	ov	298.56	0.57	2.67	0.66	161.53	1.06	156.64	0.52	1.30	1.15	2.05	0.60			
<b>147.95</b>	<b>0.76</b>	<b>-3.11</b>	<b>0.94</b>	<b>298.26</b>	<b>0.32</b>	<b>3.22</b>	<b>0.26</b>	<b>161.53</b>	<b>0.55</b>	<b>156.36</b>	<b>0.33</b>	<b>2.91</b>	<b>0.43</b>	<b>2.15</b>	<b>0.28</b>				
A42	147.77	0.75	-2.17	1.13	296.35	0.73	4.18	0.50											
	*	ov	*	ov	297.05	0.61	*												
	149.23	1.75	-3.63	1.53	296.73	0.88	3.81	1.03	157.98	0.65	157.42	0.54	0.78	0.40	*	ov			
	152.61	1.44	*	ov	298.56	0.57	2.67	0.66	161.53	1.06	156.64	0.52	1.30	1.15	2.05	0.60			
<b>147.99</b>	<b>0.69</b>	<b>-2.68</b>	<b>0.91</b>	<b>296.75</b>	<b>0.41</b>	<b>4.20</b>	<b>0.39</b>	<b>158.95</b>	<b>0.52</b>	<b>157.42</b>	<b>0.54</b>	<b>1.14</b>	<b>0.37</b>	<b>1.37</b>	<b>0.74</b>				
A43	147.80	0.92	-4.08	1.41	298.05	0.79	2.94	0.54											
	147.71	0.89	-4.68	1.26	298.66	0.74	2.47	0.54											
	148.89	2.13	-5.17	1.84	297.52	1.01	3.46	1.16	160.85	0.75	156.38	0.62	1.41	0.49	0.74	0.44			
	148.01	2.00	-4.99	1.79	297.10	1.07	4.04	1.18	161.80	1.11	157.15	0.87	2.36	1.24	1.50	0.97			
<b>147.86</b>	<b>0.58</b>	<b>-4.65</b>	<b>0.76</b>	<b>298.00</b>	<b>0.43</b>	<b>2.88</b>	<b>0.35</b>	<b>161.14</b>	<b>0.62</b>	<b>156.64</b>	<b>0.50</b>	<b>1.54</b>	<b>0.46</b>	<b>0.87</b>	<b>0.40</b>				
U44	149.32	1.01	-3.30	1.46	299.25	0.86	3.43	0.58											
	149.63	1.04	-3.65	1.44	299.07	0.84	3.17	0.60											
	149.09	2.31	-3.07	2.06	297.08	1.11	5.59	1.28	159.79	0.79	156.77	0.70	1.52	0.53	1.62	0.48			
	148.91	2.08	-2.92	1.83	297.22	0.99	5.02	1.15	160.69	0.97	155.70	0.89	2.42	1.13	0.56	1.02			
<b>149.39</b>	<b>0.66</b>	<b>-3.30</b>	<b>0.82</b>	<b>298.36</b>	<b>0.47</b>	<b>3.68</b>	<b>0.37</b>	<b>160.15</b>	<b>0.61</b>	<b>156.36</b>	<b>0.55</b>	<b>1.68</b>	<b>0.48</b>	<b>1.43</b>	<b>0.43</b>				
G45	150.77	1.95	-4.20	2.90	297.18	1.70	2.85	1.22											
	149.62	2.02	-3.94	2.70	297.91	1.63	3.22	1.23											
	150.67	4.87	-4.10	4.37	297.02	2.59	3.01	2.85	157.70	1.69	154.76	1.49	-0.78	1.27	0.67	1.21			
	148.86	3.39	-3.18	2.88	297.81	1.99	3.32	2.25	159.11	2.35	156.44	2.15	0.63	2.60	2.35	2.32			
<b>150.06</b>	<b>1.25</b>	<b>-3.82</b>	<b>1.53</b>	<b>297.55</b>	<b>0.94</b>	<b>3.06</b>	<b>0.78</b>	<b>158.18</b>	<b>1.37</b>	<b>155.30</b>	<b>1.22</b>	<b>-0.51</b>	<b>1.14</b>	<b>1.03</b>	<b>1.07</b>				
Y46	147.68	1.19	-5.32	1.72	297.62	1.05	3.66	0.75											
	147.76	1.14	-5.54	1.61	297.70	1.00	3.23	0.73											
	145.82	2.90	-3.47	2.62	297.71	1.58	3.57	1.74	158.58	0.90	157.36	0.79	1.09	0.72	2.30	0.55			
	144.70	2.29	-2.48	1.99	295.10	1.22	5.83	1.40	159.12	1.43	157.52	0.85	1.63	1.53	2.46	1.02			
<b>147.27</b>	<b>0.75</b>	<b>-4.52</b>	<b>0.94</b>	<b>297.08</b>	<b>0.58</b>	<b>3.72</b>	<b>0.47</b>	<b>158.73</b>	<b>0.76</b>	<b>157.43</b>	<b>0.58</b>	<b>1.19</b>	<b>0.65</b>	<b>2.33</b>	<b>0.48</b>				
U47	149.23	1.28	-3.44	1.82	296.79	1.05	4.60	0.71											
	148.87	1.49	-3.09	1.69	296.99	0.95	4.02	0.81											
	147.65	2.98	-1.85	2.68	297.43	1.61	3.96	1.79	156.75	0.98	157.08	0.79	1.95	0.66	1.55	0.66			
	150.41	2.02	-4.63	1.85	296.13	1.18	4.88	1.28	159.95	1.69	156.68	0.90	5.15	1.84	0.15	1.00			
<b>149.19</b>	<b>0.84</b>	<b>-3.44</b>	<b>0.96</b>	<b>296.79</b>	<b>0.57</b>	<b>4.39</b>	<b>0.47</b>	<b>157.56</b>	<b>0.85</b>	<b>156.47</b>	<b>0.59</b>	<b>2.31</b>	<b>0.62</b>	<b>1.13</b>	<b>0.55</b>				
G48	149.56	1.73	-4.02	3.15	293.30	2.10	5.60	1.10											
	150.78	2.01	-1.62	2.73	295.16	1.73	2.50	1.32											
	147.83	4.89	-2.29	4.13	295.57	2.45	3.32	3.04	157.73	1.78	154.72	1.35	0.66	0.97	2.44	0.99			
	152.80	3.41	-3.64	2.87	296.21	1.60	1.45	1.95	159.68	2.22	158.88	1.42	2.60	2.68	6.60	1.70			
<b>150.28</b>	<b>1.19</b>	<b>-2.89</b>	<b>1.55</b>	<b>295.21</b>	<b>0.95</b>	<b>3.85</b>	<b>0.75</b>	<b>158.49</b>	<b>1.39</b>	<b>156.69</b>	<b>0.98</b>	<b>0.89</b>	<b>0.91</b>	<b>3.49</b>	<b>0.85</b>				
A49	150.87	1.99	-5.25	3.03	295.69	1.83	2.84	1.17											
	147.91	2.31	-2.75	2.71	295.62	1.67	3.46	1.45											
	150.61	4.54	-4.99	3.92	296.64	2.33	1.89	2.72	162.73	1.56	155.83	1.34	2.90	1.07	1.85	1.10			
	151.26	2.97	-6.10	2.62	296.15	1.50	2.93	1.72	157.27	2.11	157.03	1.16	-2.55	2.40	3.06	1.39			





Table D

Tab. D	JC4'H4'	Δ	JC4'H5'+ JC4'H5''	Δ	JC5'H5'+ JC5'H5''	Δ	JC5'H4'	Δ	JC5'H5'- JH5'H5''	Δ	JC5'H5'- JH5'H5''	Δ	JH5'H4'	Δ	JH5'H4'	Δ	JH5'H5''	JC5'H5'	JC5'H5''
G38	*		ov	*	ov	280.93	3.26	1.08	ov										
	*		ov	*	ov	280.26	3.68	4.67	3.08										
	162.76	2.14	*	ov	277.06	2.89	4.95	3.49	162.38	1.11	164.37	1.32	5.76	0.88	2.29	1.08			
	*		ov	-4.90	1.50	280.24	2.43	4.69	3.16	161.49	0.99	162.97	0.88	4.87	1.20	0.89	1.17		
	<b>162.76</b>	<b>2.14</b>	<b>-4.90</b>	<b>1.50</b>	<b>279.55</b>	<b>1.48</b>	<b>4.76</b>	<b>1.86</b>	<b>161.88</b>	<b>0.74</b>	<b>163.40</b>	<b>0.74</b>	<b>5.45</b>	<b>0.71</b>	<b>1.64</b>	<b>0.79</b>	-22.87	139.01	140.53
G39	163.96	0.85	-2.78	1.03	287.69	1.74	1.54	1.44											
	165.19	0.91	-5.45	1.12	288.00	1.61	3.46	1.32											
	165.29	0.99	-4.11	0.80	283.11	1.27	6.12	1.60	157.30	0.66	164.54	0.59	1.44	0.52	-0.44	0.49			
	164.64	1.11	-4.90	0.91	286.54	1.30	4.92	1.59	156.37	0.47	164.52	0.43	0.51	0.62	-0.46	0.54			
	<b>164.72</b>	<b>0.48</b>	<b>-4.28</b>	<b>0.47</b>	<b>285.92</b>	<b>0.72</b>	<b>3.84</b>	<b>0.74</b>	<b>156.69</b>	<b>0.38</b>	<b>164.53</b>	<b>0.35</b>	<b>1.05</b>	<b>0.40</b>	<b>-0.45</b>	<b>0.36</b>	-17.65	139.04	146.88
C40	154.10	ov	9.28	ov	295.24	ov	-2.49	ov											
	156.20	0.67	-3.01	0.80	283.23	1.02	1.27	1.02											
	164.60	ov	-1.22	0.45	283.56	0.73	9.19	ov	159.70	ov	174.33	0.46	1.16	ov	-2.45	0.39			
	156.89	0.75	-3.70	0.60	279.86	1.12	4.64	1.12	164.23	0.28	175.56	0.39	5.69	ov	-1.22	0.46			
	<b>156.50</b>	<b>0.50</b>	<b>-2.25</b>	<b>0.33</b>	<b>282.66</b>	<b>0.52</b>	<b>2.80</b>	<b>0.75</b>	<b>164.23</b>	<b>0.28</b>	<b>175.04</b>	<b>0.29</b>	ov	ov	<b>-1.93</b>	<b>0.29</b>	-28.31	135.93	146.74
A43	161.25	3.07	-0.49	5.19	262.15	4.01	4.23	2.39											
	159.84	3.09	-0.54	4.29	254.85	ov	9.69	ov											
	157.98	7.38	2.78	ov	262.28	4.03	4.09	5.15	161.47	ov	184.11	3.14	*	ov	7.51	2.29			
	164.20	6.38	-4.90	5.64	262.29	4.31	2.25	4.77	151.46	2.96	183.29	2.88	2.61	3.92	6.69	3.59			
	<b>160.72</b>	<b>1.99</b>	<b>-1.64</b>	<b>2.85</b>	<b>262.23</b>	<b>2.37</b>	<b>3.87</b>	<b>1.98</b>	<b>151.46</b>	<b>2.96</b>	<b>183.66</b>	<b>2.12</b>	<b>2.61</b>	<b>3.92</b>	<b>7.28</b>	<b>1.93</b>	-36.44	115.02	147.22
U44	169.96	2.13	1.42	2.52	265.94	3.76	5.84	3.17											
	172.45	1.40	-1.57	1.73	259.06	2.47	7.48	1.98											
	172.37	2.82	-0.99	2.48	260.96	3.44	10.81	3.99	165.17	1.47	180.27	0.87	4.79	1.15	7.86	0.69			
	171.24	1.89	-0.36	1.59	269.36	2.43	7.18	2.85	163.89	2.24	179.76	0.92	3.52	2.42	7.35	1.07			
	<b>171.66</b>	<b>0.94</b>	<b>-0.58</b>	<b>0.98</b>	<b>260.49</b>	<b>1.43</b>	<b>7.49</b>	<b>1.36</b>	<b>164.78</b>	<b>1.23</b>	<b>180.03</b>	<b>0.63</b>	<b>4.56</b>	<b>1.04</b>	<b>7.71</b>	<b>0.58</b>	-42.16	122.62	137.87
G45	169.65	3.30	-0.08	4.08	276.94	6.84	-5.70	5.65											
	175.09	3.15	-2.65	3.95	262.04	5.75	7.99	4.60											
	175.28	ov	-5.71	ov	264.40	5.94	6.83	7.08	168.14	2.36	180.25	2.13	1.72	1.92	5.43	1.80			
	173.40	3.59	-0.96	2.68	271.02	3.90	-0.99	5.20	171.19	1.77	180.15	1.46	4.77	2.24	5.33	1.85			
	<b>172.75</b>	<b>1.92</b>	<b>-1.17</b>	<b>1.95</b>	<b>268.73</b>	<b>2.62</b>	<b>2.20</b>	<b>2.72</b>	<b>170.09</b>	<b>1.42</b>	<b>180.18</b>	<b>1.21</b>	<b>3.02</b>	<b>1.46</b>	<b>5.38</b>	<b>1.29</b>	-40.77	129.32	139.41
Y46	162.37	2.17	3.08	2.73	267.52	4.33	6.40	3.62											
	164.38	2.14	-2.08	2.73	269.44	4.14	6.74	3.37											
	166.16	2.86	-0.71	2.32	269.93	3.53	3.99	4.26	175.70	1.60	168.59	1.32	3.49	1.17	8.14	1.00			
	164.70	2.74	-2.40	2.16	268.74	3.55	7.44	4.29	168.59	1.40	165.49	1.37	3.17	1.78	5.04	1.62			
	<b>164.14</b>	<b>1.21</b>	<b>-0.77</b>	<b>1.22</b>	<b>269.00</b>	<b>1.92</b>	<b>6.23</b>	<b>1.91</b>	<b>171.67</b>	<b>1.06</b>	<b>167.10</b>	<b>0.95</b>	<b>3.40</b>	<b>0.98</b>	<b>7.29</b>	<b>0.85</b>	-34.88	136.79	132.22
U47	161.60	1.94	-0.81	2.28	272.21	3.47	5.17	2.93											
	160.93	1.80	0.21	2.04	273.70	3.49	2.83	3.15											
	164.19	2.33	-3.40	2.00	273.11	3.09	4.26	3.61	178.96	1.50	163.60	1.17	5.93	1.27	4.15	1.05			
	163.75	2.02	-2.61	1.79	270.01	2.86	6.52	3.23	178.49	1.20	164.13	0.92	5.46	1.44	4.68	1.06			
	<b>162.39</b>	<b>1.00</b>	<b>-1.78</b>	<b>1.00</b>	<b>272.08</b>	<b>1.60</b>	<b>4.71</b>	<b>1.60</b>	<b>178.67</b>	<b>0.94</b>	<b>163.93</b>	<b>0.72</b>	<b>5.72</b>	<b>0.95</b>	<b>4.41</b>	<b>0.74</b>	-35.26	143.41	128.66
G48	154.45	2.29	-0.36	2.54	271.75	ov	4.62	3.98											
	153.82	2.14	-0.21	2.35	276.92	3.52	4.10	3.13											
	151.62	ov	2.47	ov	268.90	ov	7.47	ov	156.32	1.39	169.25	1.13	8.59	1.21	5.58	1.04			
	155.11	2.31	-1.50	2.11	276.10	3.38	2.92	3.74	154.31	1.21	170.64	1.24	6.58	1.39	7.17	1.32			
	<b>154.42</b>	<b>1.30</b>	<b>-0.77</b>	<b>1.33</b>	<b>277.53</b>	<b>2.44</b>	<b>3.68</b>	<b>2.06</b>	<b>155.17</b>	<b>0.91</b>	<b>169.97</b>	<b>0.84</b>	<b>7.72</b>	<b>0.91</b>	<b>6.19</b>	<b>0.82</b>	-23.80	131.37	146.17
A49	159.88	1.99	-6.75	ov	278.44	ov	8.70	ov											
	158.68	1.90	-4.21	2.03	285.64	3.46	3.99	3.23											
	161.74	2.25	-8.61	ov	274.26	ov	12.88	ov	156.16	1.30	168.70	1.24	0.05	1.10	5.36	1.18			
	161.37	1.87	-6.90	1.73	285.49	2.89	4.14	3.14	155.28	0.89	168.14	1.02	-0.83	1.13	4.80	1.10			
	<b>160.33</b>	<b>0.99</b>	<b>-5.77</b>	<b>1.32</b>	<b>285.55</b>	<b>2.22</b>	<b>4.07</b>	<b>2.25</b>	<b>155.56</b>	<b>0.74</b>	<b>168.36</b>	<b>0.79</b>	<b>-0.38</b>	<b>0.79</b>	<b>5.06</b>	<b>0.80</b>	-19.18	136.37	149.18
A50	159.72	1.08	-1.43	1.64	298.24	2.84	-0.05	1.84											
	160.34	1.34	-1.37	1.49	292.90	ov	5.24	ov											
	160.09	2.10	-1.80	1.69	298.28	3.02	-0.08	3.71	155.43	0.92	168.35	0.83	1.97	0.60	6.31	0.74			
	162.20	1.26	-3.22	1.08	298.46	1.85	-0.31	2.16	156.70	0.92	169.09	0.64	3.24	1.16	7.04	0.75			
	<b>160.60</b>	<b>0.66</b>	<b>-2.24</b>	<b>0.70</b>	<b>298.37</b>	<b>1.38</b>	<b>-0.15</b>	<b>1.31</b>	<b>156.07</b>	<b>0.65</b>	<b>168.81</b>	<b>0.51</b>	<b>2.24</b>	<b>0.53</b>	<b>6.67</b>	<b>0.53</b>	-13.26	142.81	155.56
A51	159.67	2.12	-3.16	2.67	289.44	4.25	0.47	3.32											
	156.59	2.42	-2.03	2.73	291.03	4.50	2.82	3.92											
	157.39	2.89	-0.88	2.39	287.87	4.27	2.03	5.03	164.59	1.56	163.42	1.53	3.41	1.20	5.22	1.31			
	154.60	ov	-0.04	2.01	279.36	4.39	14.49	4.91	164.82	1.44	162.01	1.10	3.65	1.75	3.81	1.36			
	<b>158.11</b>	<b>1.40</b>	<b>-1.26</b>	<b>1.20</b>	<b>286.93</b>	<b>2.17</b>	<b>3.83</b>	<b>2.06</b>	<b>164.71</b>	<b>1.06</b>	<b>162.49</b>	<b>0.89</b>	<b>3.49</b>	<b>0.99</b>	<b>4.54</b>	<b>0.94</b>	-20.14	144.58	142.35
A52	155.69	1.95	-0.93	2.38	283.05	ov	7.33	ov											
	154.91	2.48	0.46	2.72	289.51	4.93	2.25	4.50											
	156.21	2.65	-1.45	2.28	293.80	4.36	-3.42	5.08	162.58	1.27	161.39	1.44	2.69	1.05	2.13	1.28			
	155.03	1.98	0.34	1.63	280.59	ov	11.17	ov	159.73	1.64	152.12	0.86	-0.16	1.79	-7.14	1.08			
	<b>155.42</b>	<b>1.10</b>	<b>-0.29</b>	<b>1.07</b>	<b>291.92</b>	<b>3.26&lt;/</b>													

Table E

Tab. E	JCaHa	Δ	JCaH2+ JCaH3	Δ	JCrH2+ JCrH3	Δ	JCrHa	Δ	JCrH2- JH2H3	Δ	JCrH3- JH2H3	Δ	JH2Ha	Δ	JH2Ha	Δ	JH2H3	JCrH2	JCrH3
<b>y3</b>																			
J+D	117.71	0.35	-5.23	0.36	277.96	0.18	-6.52	0.17	178.73	0.30	112.24	0.64	6.32	0.28	6.09	0.57	-6.50	172.23	105.73
J	145.26	0.62	-8.31	0.80	255.78	0.43	-4.17	0.36	141.26	0.65	141.39	0.65	1.95	0.48	11.81	0.66	-13.43	127.82	127.96
D	<b>-27.55</b>	<b>0.71</b>	<b>3.07</b>	<b>0.87</b>	<b>22.18</b>	<b>0.47</b>	<b>-2.35</b>	<b>0.40</b>	<b>37.47</b>	<b>0.71</b>	<b>-29.16</b>	<b>0.91</b>	<b>4.37</b>	<b>0.55</b>	<b>-5.73</b>	<b>0.88</b>	<b>6.93</b>	<b>44.40</b>	<b>-22.23</b>
<b>n8</b>																			
J+D	127.82	0.10	-14.57	0.11	275.79	0.05	-6.94	0.05	142.22	0.07	149.75	0.08	5.82	0.07	0.62	0.07	-8.09	134.13	141.66
J	140.46	0.10	-10.94	0.12	260.63	0.06	-4.86	0.06	146.20	0.08	145.68	0.08	7.07	0.07	6.09	0.08	-15.63	130.57	130.06
D	<b>-12.65</b>	<b>0.14</b>	<b>-3.63</b>	<b>0.16</b>	<b>15.16</b>	<b>0.08</b>	<b>-2.09</b>	<b>0.08</b>	<b>-3.97</b>	<b>0.10</b>	<b>4.07</b>	<b>0.11</b>	<b>-1.25</b>	<b>0.10</b>	<b>-5.47</b>	<b>0.10</b>	<b>7.54</b>	<b>3.56</b>	<b>11.60</b>
<b>d22</b>																			
J+D	124.76	0.21	-10.37	0.26	294.45	0.13	-5.79	0.10	137.96	0.16	110.44	0.33	-2.96	0.16	2.20	0.18	23.03	160.99	133.47
J	140.10	0.33	-6.89	0.40	260.80	0.21	-3.72	0.18	149.12	0.31	143.20	0.29	3.99	0.29	2.13	0.21	-15.76	133.36	127.44
D	<b>-15.33</b>	<b>0.39</b>	<b>-3.48</b>	<b>0.48</b>	<b>33.65</b>	<b>0.25</b>	<b>-2.07</b>	<b>0.20</b>	<b>-11.17</b>	<b>0.35</b>	<b>-32.76</b>	<b>0.44</b>	<b>-6.95</b>	<b>0.33</b>	<b>0.07</b>	<b>0.28</b>	<b>38.79</b>	<b>27.62</b>	<b>6.03</b>
<b>f30</b>																			
J+D	128.48	0.43	-14.43	0.50	253.22	0.26	-8.21	0.21	171.43	0.53	142.93	0.51	-0.76	0.46	7.44	0.43	-30.57	140.86	112.36
J	143.56	0.31	-9.10	0.55	258.15	0.29	-5.30	0.18	143.88	0.43	146.55	0.46	0.75	0.25	11.33	0.30	-16.14	127.74	130.41
D	<b>-15.09</b>	<b>0.53</b>	<b>-5.33</b>	<b>0.75</b>	<b>-4.93</b>	<b>0.39</b>	<b>-2.91</b>	<b>0.28</b>	<b>27.55</b>	<b>0.69</b>	<b>-3.61</b>	<b>0.69</b>	<b>-1.51</b>	<b>0.52</b>	<b>-3.90</b>	<b>0.53</b>	<b>-14.43</b>	<b>13.12</b>	<b>-18.05</b>
<b>n35</b>																			
J+D	192.70	0.09	-13.46	0.22	284.54	0.11	-5.27	0.04	137.80	0.11	139.67	0.47	5.72	0.06	4.50	0.06	3.53	141.33	143.20
J	150.87	0.06	-10.12	0.12	262.12	0.06	-4.92	0.03	147.78	0.06	145.73	0.04	7.92	0.04	7.15	0.05	-15.70	132.08	130.03
D	<b>41.84</b>	<b>0.11</b>	<b>-3.34</b>	<b>0.25</b>	<b>22.42</b>	<b>0.13</b>	<b>-0.35</b>	<b>0.06</b>	<b>-9.98</b>	<b>0.13</b>	<b>-6.06</b>	<b>0.48</b>	<b>-2.20</b>	<b>0.07</b>	<b>-2.64</b>	<b>0.08</b>	<b>19.23</b>	<b>9.25</b>	<b>13.17</b>
<b>d36</b>																			
J+D	143.20	0.24	1.52	0.40	229.51	0.19	-0.11	0.12	151.62	0.23		ov	14.50	0.20	17.16	0.18			
J	149.47	0.11	-7.53	0.21	256.43	0.11	-5.49	0.07	143.90	0.11	150.45	ov	2.25	0.09	11.40	0.08	-18.96	124.94	131.49
D	<b>-6.27</b>	<b>0.27</b>	<b>9.05</b>	<b>0.45</b>	<b>-26.92</b>	<b>0.22</b>	<b>5.38</b>	<b>0.14</b>	<b>7.71</b>	<b>0.25</b>		ov	<b>12.24</b>	<b>0.22</b>	<b>5.76</b>	<b>0.20</b>			
<b>n37</b>																			
J+D	114.96	0.28	-14.52	0.28	224.44	0.16	-7.61	0.15	154.03	0.18	135.14	0.40	-4.80	0.17	7.67	0.40	-32.36	121.67	102.77
J	140.21	0.20	-10.46	0.20	263.21	0.11	-5.45	0.11	149.12	0.14	144.12	0.15	1.94	0.15	12.27	0.15	-15.01	134.11	129.10
D	<b>-25.25</b>	<b>0.34</b>	<b>-4.06</b>	<b>0.35</b>	<b>-38.77</b>	<b>0.19</b>	<b>-2.15</b>	<b>0.19</b>	<b>4.91</b>	<b>0.23</b>	<b>-8.98</b>	<b>0.43</b>	<b>-6.73</b>	<b>0.22</b>	<b>-4.59</b>	<b>0.43</b>	<b>-17.35</b>	<b>-12.44</b>	<b>-26.33</b>
<b>d40</b>																			
J+D	157.47	0.07	-8.28	0.08	261.89	0.04	-0.34	0.03	156.64	0.05	123.91	0.07	17.41	0.04	4.00	0.07	-9.33	147.31	114.58
J	140.89	0.09	-10.63	0.11	261.56	0.06	-4.06	0.05	147.07	0.08	145.83	0.08	10.18	0.06	3.64	0.07	-15.67	131.40	130.16
D	<b>16.58</b>	<b>0.11</b>	<b>2.35</b>	<b>0.14</b>	<b>0.33</b>	<b>0.07</b>	<b>3.72</b>	<b>0.06</b>	<b>9.57</b>	<b>0.09</b>	<b>-21.92</b>	<b>0.11</b>	<b>7.22</b>	<b>0.07</b>	<b>0.36</b>	<b>0.10</b>	<b>6.34</b>	<b>15.91</b>	<b>-15.58</b>
<b>w43</b>																			
J+D	135.14	0.51	-7.34	0.90	296.16	0.45	-7.61	0.25	144.98	0.84	104.17	0.85	-0.88	0.36	6.64	0.75	23.50	168.48	127.67
J	145.43	0.37	-7.21	1.34	254.78	0.64	-4.05	0.21	142.01	1.67	147.12	0.75	1.78	0.31	11.13	0.33	-17.18	124.83	129.94
D	<b>-10.29</b>	<b>0.63</b>	<b>-0.12</b>	<b>1.61</b>	<b>41.38</b>	<b>0.78</b>	<b>-3.56</b>	<b>0.33</b>	<b>2.97</b>	<b>1.87</b>	<b>-42.95</b>	<b>1.14</b>	<b>-2.66</b>	<b>0.48</b>	<b>-4.50</b>	<b>0.82</b>	<b>40.68</b>	<b>43.65</b>	<b>-2.27</b>
<b>y45</b>																			
J+D	129.95	0.35	-18.07	0.46	236.79	0.21	-6.96	0.17	164.54	0.41	152.88	0.44	6.40	0.31	-1.32	0.31	-40.32	124.22	112.56
J	142.97	0.41	-12.04	1.23	265.39	0.63	-3.84	0.23	142.97	1.52	146.41	0.72	11.18	0.40	4.41	0.38	-11.99	130.97	134.41
D	<b>-13.02</b>	<b>0.54</b>	<b>-6.03</b>	<b>1.32</b>	<b>-28.60</b>	<b>0.67</b>	<b>-3.12</b>	<b>0.29</b>	<b>21.57</b>	<b>1.57</b>	<b>6.47</b>	<b>0.85</b>	<b>-4.78</b>	<b>0.51</b>	<b>-5.73</b>	<b>0.49</b>	<b>-28.32</b>	<b>-6.75</b>	<b>-21.85</b>
<b>d46</b>																			
J+D	138.63	0.19	-15.60	0.22	299.49	0.10	-6.38	0.09	107.63	0.28	150.17	0.13	8.25	0.21	-3.12	0.12	20.85	128.47	171.02
J	143.13	0.18	-11.48	0.29	262.13	0.16	-3.82	0.10	145.74	0.20	146.00	0.23	11.81	0.13	3.41	0.15	-14.81	130.93	131.19
D	<b>-4.50</b>	<b>0.26</b>	<b>-4.12</b>	<b>0.37</b>	<b>37.37</b>	<b>0.19</b>	<b>-2.56</b>	<b>0.13</b>	<b>-38.11</b>	<b>0.34</b>	<b>4.17</b>	<b>0.27</b>	<b>-3.55</b>	<b>0.24</b>	<b>-6.54</b>	<b>0.19</b>	<b>35.65</b>	<b>-2.46</b>	<b>39.82</b>
<b>d47</b>																			
J+D	126.39	0.15	-15.38	0.16	265.77	0.08	-8.63	0.07	135.34	0.12	164.80	0.11	5.86	0.11	0.22	0.10	-17.18	118.15	147.62
J	147.99	0.14	-10.98	0.17	264.11	0.09	-5.32	0.08	146.31	0.10	142.61	0.13	11.10	0.09	3.58	0.11	-12.41	133.90	130.20
D	<b>-21.61</b>	<b>0.20</b>	<b>-4.40</b>	<b>0.23</b>	<b>1.67</b>	<b>0.12</b>	<b>-3.32</b>	<b>0.11</b>	<b>-10.98</b>	<b>0.16</b>	<b>22.19</b>	<b>0.17</b>	<b>-5.24</b>	<b>0.15</b>	<b>-3.36</b>	<b>0.15</b>	<b>-4.77</b>	<b>-15.75</b>	<b>17.42</b>
<b>f52</b>																			
J+D	136.01	0.49	-12.83	0.54	295.17	0.28	-6.94	0.25		ov		ov		ov		ov	-4.18		
J	145.50	0.37	-8.11	0.59	259.46	0.30	-3.83	0.21	143.29	1.06	141.80	0.36	10.68	0.31	2.01	0.38	-12.81	130.47	128.99
D	<b>-9.49</b>	<b>0.62</b>	<b>-4.72</b>	<b>0.80</b>	<b>35.72</b>	<b>0.41</b>	<b>-3.10</b>	<b>0.33</b>		ov		ov		ov		ov	<b>-6.19</b>	<b>0.78</b>	

Table F

Tab. F	JC4'H4'	Δ	JC4'H5'+ JC4'H5''	Δ	JC5'H5'+ JC5'H5''	Δ	JC5'H4'	Δ	JC5'H5'- JH5'H5''	Δ	JC5'H5'- JH5'H5''	Δ	JH5'H4'	Δ	JH5'H4'	Δ	JH5'H5''	JC5'H5'	JC5'H5''
<b>G38</b>																			
J+D	162.76	2.14	-4.90	1.50	279.55	1.48	4.76	1.86	161.88	0.74	163.40	0.74	5.45	0.71	1.64	0.79	-22.87	139.01	140.53
J	148.39	1.16	-5.24	1.82	296.27	0.68	3.42	0.59	157.89	0.91	156.96	1.03	1.00	0.70	2.32	0.91	-9.29	148.60	147.67
D	<b>14.37</b>	<b>2.43</b>	<b>0.34</b>	<b>2.36</b>	<b>-16.72</b>	<b>1.63</b>	<b>1.34</b>	<b>1.95</b>	<b>3.99</b>	<b>1.17</b>	<b>6.44</b>	<b>1.26</b>	<b>4.44</b>	<b>1.00</b>	<b>-0.68</b>	<b>1.20</b>	<b>-13.58</b>	<b>-9.59</b>	<b>-7.14</b>
<b>G39</b>																			
J+D	164.72	0.48	-4.28	0.47	285.92	0.72	3.84	0.74	156.69	0.38	164.53	0.35	1.05	0.40	-0.45	0.36	-17.65	139.04	146.88
J	149.03	0.81	-2.82	0.96	296.86	0.43	2.85	0.36	159.12	0.58	156.52	0.57	0.47	0.48	3.31	0.47	-9.39	149.73	147.13
D	<b>15.70</b>	<b>0.94</b>	<b>-1.46</b>	<b>1.07</b>	<b>-10.94</b>	<b>0.84</b>	<b>0.99</b>	<b>0.82</b>	<b>-2.42</b>	<b>0.69</b>	<b>8.01</b>	<b>0.67</b>	<b>0.59</b>	<b>0.62</b>	<b>-3.76</b>	<b>0.59</b>	<b>-8.26</b>	<b>-10.69</b>	<b>-0.26</b>
<b>C40</b>																			
J+D	156.50	0.50	-2.25	0.33	282.66	0.52	2.80	0.75	164.23	0.28	175.04	0.29	ov	ov	-1.93	0.29	-28.31	135.93	146.74
J	150.14	0.52	-5.41	0.62	297.27	0.37	0.59	1.24	160.08	0.54	156.39	0.42	1.80	0.46	1.65	0.35	-9.60	150.48	146.79
D	<b>6.36</b>	<b>0.72</b>	<b>3.16</b>	<b>0.70</b>	<b>-14.61</b>	<b>0.64</b>	<b>2.21</b>	<b>1.45</b>	<b>4.15</b>	<b>0.60</b>	<b>18.65</b>	<b>0.51</b>	ov	ov	<b>-3.59</b>	<b>0.45</b>	<b>-18.71</b>	<b>-14.55</b>	<b>-0.05</b>
<b>A43</b>																			
J+D	160.72	1.99	-1.64	2.85	262.23	2.37	3.87	1.98	151.46	2.96	183.66	2.12	2.61	3.92	7.28	1.93	-36.44	115.02	147.22
J	147.86	0.58	-4.65	0.76	298.00	0.43	2.88	0.35	161.14	0.62	156.64	0.50	1.54	0.46	0.87	0.40	-9.89	151.25	146.75
D	<b>12.86</b>	<b>2.07</b>	<b>3.00</b>	<b>2.95</b>	<b>-35.77</b>	<b>2.41</b>	<b>0.98</b>	<b>2.01</b>	<b>-9.68</b>	<b>3.02</b>	<b>27.02</b>	<b>2.18</b>	<b>1.07</b>	<b>3.94</b>	<b>6.40</b>	<b>1.98</b>	<b>-26.56</b>	<b>-36.24</b>	<b>0.47</b>
<b>U44</b>																			
J+D	171.66	0.94	-0.58	0.98	260.49	1.43	7.49	1.36	164.78	1.23	180.03	0.63	4.56	1.04	7.71	0.58	-42.16	122.62	137.87
J	149.39	0.66	-3.30	0.82	298.36	0.47	3.68	0.37	160.15	0.61	156.36	0.55	1.68	0.48	1.43	0.43	-9.08	151.08	147.28
D	<b>22.27</b>	<b>1.14</b>	<b>2.72</b>	<b>1.27</b>	<b>-37.87</b>	<b>1.51</b>	<b>3.81</b>	<b>1.41</b>	<b>4.63</b>	<b>1.38</b>	<b>23.67</b>	<b>0.84</b>	<b>2.88</b>	<b>1.14</b>	<b>6.28</b>	<b>0.72</b>	<b>-33.09</b>	<b>-28.46</b>	<b>-9.42</b>
<b>G45</b>																			
J+D	172.75	1.92	-1.17	1.95	268.73	2.62	2.20	2.72	170.09	1.42	180.18	1.21	3.02	1.46	5.38	1.29	-40.77	129.32	139.41
J	150.06	1.25	-3.82	1.53	297.55	0.94	3.06	0.78	158.18	1.37	155.30	1.22	-0.51	1.14	1.03	1.07	-7.97	150.21	147.33
D	<b>22.69</b>	<b>2.30</b>	<b>2.65</b>	<b>2.48</b>	<b>-28.81</b>	<b>2.78</b>	<b>-0.86</b>	<b>2.83</b>	<b>11.91</b>	<b>1.97</b>	<b>24.88</b>	<b>1.72</b>	<b>3.52</b>	<b>1.85</b>	<b>4.35</b>	<b>1.68</b>	<b>-32.81</b>	<b>-20.89</b>	<b>-7.92</b>
<b>Y46</b>																			
J+D	164.14	1.21	-0.77	1.22	269.00	1.92	6.23	1.91	171.67	1.06	167.10	0.95	3.40	0.98	7.29	0.85	-34.88	136.79	132.22
J	147.27	0.75	-4.52	0.94	297.08	0.58	3.72	0.47	158.73	0.76	157.43	0.58	1.19	0.65	2.33	0.48	-9.54	149.19	147.89
D	<b>16.86</b>	<b>1.42</b>	<b>3.75</b>	<b>1.54</b>	<b>-28.08</b>	<b>2.01</b>	<b>2.51</b>	<b>1.97</b>	<b>12.94</b>	<b>1.30</b>	<b>9.67</b>	<b>1.11</b>	<b>2.21</b>	<b>1.17</b>	<b>4.95</b>	<b>0.98</b>	<b>-25.34</b>	<b>-12.41</b>	<b>-15.67</b>
<b>U47</b>																			
J+D	162.39	1.00	-1.78	1.00	272.08	1.60	4.71	1.60	178.67	0.94	163.93	0.72	5.72	0.95	4.41	0.74	-35.26	143.41	128.66
J	149.19	0.84	-3.44	0.96	296.79	0.57	4.39	0.47	157.56	0.85	156.47	0.59	2.31	0.62	1.13	0.55	-8.62	148.94	147.85
D	<b>13.20</b>	<b>1.30</b>	<b>1.66</b>	<b>1.39</b>	<b>-24.71</b>	<b>1.69</b>	<b>0.32</b>	<b>1.67</b>	<b>21.11</b>	<b>1.26</b>	<b>7.45</b>	<b>0.94</b>	<b>3.41</b>	<b>1.13</b>	<b>3.28</b>	<b>0.93</b>	<b>-26.64</b>	<b>-5.53</b>	<b>-19.19</b>
<b>G48</b>																			
J+D	154.42	1.30	-0.77	1.33	277.53	2.44	3.88	2.06	155.17	0.91	169.97	0.84	7.72	0.91	6.19	0.82	-23.80	131.37	146.17
J	150.28	1.19	-2.89	1.55	295.21	0.95	3.85	0.75	158.49	1.39	156.69	0.98	0.89	0.91	3.49	0.85	-9.98	148.51	146.70
D	<b>4.15</b>	<b>1.76</b>	<b>2.12</b>	<b>2.05</b>	<b>-17.67</b>	<b>2.61</b>	<b>0.04</b>	<b>2.19</b>	<b>-3.32</b>	<b>1.66</b>	<b>13.28</b>	<b>1.29</b>	<b>6.84</b>	<b>1.29</b>	<b>2.69</b>	<b>1.18</b>	<b>-13.82</b>	<b>-17.14</b>	<b>-0.50</b>
<b>A49</b>																			
J+D	160.33	0.99	-5.77	1.32	285.55	2.22	4.07	2.25	155.56	0.74	168.36	0.79	-0.38	0.79	5.06	0.80	-19.18	136.37	149.18
J	150.00	1.29	-4.74	1.48	295.97	0.88	2.96	0.77	160.80	1.26	156.52	0.87	2.00	0.98	2.32	0.86	-10.67	150.12	145.84
D	<b>10.33</b>	<b>1.63</b>	<b>-1.03</b>	<b>1.98</b>	<b>-10.42</b>	<b>2.39</b>	<b>1.10</b>	<b>2.38</b>	<b>-5.24</b>	<b>1.46</b>	<b>11.84</b>	<b>1.18</b>	<b>-2.38</b>	<b>1.26</b>	<b>2.75</b>	<b>1.18</b>	<b>-8.51</b>	<b>-13.75</b>	<b>3.34</b>
<b>A50</b>																			
J+D	160.60	0.66	-2.24	0.70	298.37	1.38	-0.15	1.31	156.07	0.65	168.81	0.51	2.24	0.53	6.67	0.53	-13.26	142.81	155.56
J	152.51	0.51	-3.29	0.60	295.49	0.37	-0.26	0.31	158.83	0.50	157.79	0.44	1.82	0.36	5.14	0.42	-10.56	148.27	147.22
D	<b>8.08</b>	<b>0.84</b>	<b>1.06</b>	<b>0.93</b>	<b>2.88</b>	<b>1.43</b>	<b>0.11</b>	<b>1.35</b>	<b>-2.76</b>	<b>0.82</b>	<b>11.03</b>	<b>0.67</b>	<b>0.42</b>	<b>0.64</b>	<b>1.53</b>	<b>0.67</b>	<b>-2.69</b>	<b>-5.45</b>	<b>8.34</b>
<b>A51</b>																			
J+D	158.11	1.40	-1.26	1.20	286.93	2.17	3.83	2.06	164.71	1.06	162.49	0.89	3.49	0.99	4.54	0.94	-20.14	144.58	142.35
J	150.31	1.37	-4.20	1.65	296.71	0.98	2.57	0.82	160.17	1.38	158.11	1.17	2.67	0.95	3.20	1.01	-10.79	149.38	147.32
D	<b>7.80</b>	<b>1.96</b>	<b>2.93</b>	<b>2.04</b>	<b>-9.78</b>	<b>2.39</b>	<b>1.26</b>	<b>2.21</b>	<b>4.54</b>	<b>1.74</b>	<b>4.37</b>	<b>1.47</b>	<b>0.82</b>	<b>1.37</b>	<b>1.34</b>	<b>1.38</b>	<b>-9.35</b>	<b>-4.81</b>	<b>-4.97</b>
<b>A52</b>																			
J+D	155.42	1.10	-0.29	1.07	291.92	3.26	-0.24	3.37	161.51	1.01	154.55	0.74	1.97	0.91	-3.28	0.83	-12.07	149.44	142.48
J	150.43	0.99	-3.91	1.13	296.36	0.68	2.11	0.60	158.24	1.04	155.57	0.86	1.06	0.85	2.41	0.78	-8.72	149.51	146.85
D	<b>4.99</b>	<b>1.48</b>	<b>3.62</b>	<b>1.55</b>	<b>-4.45</b>	<b>3.34</b>	<b>-2.35</b>	<b>3.42</b>	<b>3.27</b>	<b>1.45</b>	<b>-1.02</b>	<b>1.13</b>	<b>0.90</b>	<b>1.24</b>	<b>-5.68</b>	<b>1.14</b>	<b>-3.35</b>	<b>-0.07</b>	<b>-4.37</b>
<b>A53</b>																			
J+D	161.80	1.60	-3.77	1.46	282.64	2.00	2.49	1.97	154.14	0.97	171.67	1.08	6.03	1.03	3.17	1.13	-21.59	132.56	150.08
J	152.09	1.06	-3.81	1.32	296.50	0.81	3.13	0.67	160.12	0.96	158.96	1.04	2.52	0.79	2.48	0.85	-11.29	148.83	147.67
D	<b>9.71</b>	<b>1.92</b>	<b>0.04</b>	<b>1.96</b>	<b>-13.86</b>	<b>2.16</b>	<b>-0.64</b>	<b>2.08</b>	<b>-5.98</b>	<b>1.36</b>	<b>12.70</b>	<b>1.50</b>	<b>3.51</b>	<b>1.29</b>	<b>0.69</b>	<b>1.41</b>	<b>-10.30</b>	<b>-16.27</b>	<b>2.47</b>
<b>G57</b>																			
J+D	162.04	0.76	-2.30	0.81	266.18	0.93	5.58	0.95	168.91	0.50	172.50	0.50	4.50	0.52	5.15	0.53	-37.62	131.30	134.88
J	150.07	0.98	-5.62	1.36	296.43	0.53	3.71	0.40	159.10										

**References**

- Ding, K. Y. and Gronenborn, A. M. (2003) *J. Magn. Reson.* 163, 208-214.
- Harbison, G. S. (1993) *J. Am. Chem. Soc.* 115, 3026-3027.
- Kumar, A., Grace, R. C. R. and Madhu, P. K. (2000) *Prog. Nucl. Magn. Reson. Spectrosc.* 37, 191-319.
- Meissner, A., Schulte-Herbruggen, T., Briand, J. and Sorensen, O. W. (1998) *Mol. Phys.* 95, 1137-1142.
- Miclet, E., O'Neil-Cabello, E., Nikonowicz, E. P., Live, D. and Bax, A. (2003) *J. Am. Chem. Soc.* 125, 15740-15741.
- Miclet, E., Williamson, D. C., Clore, G. M., Bryce, D. L. and Bax, A. (2004) *J. Am. Chem. Soc.* 126, 10560-10570.
- Nicholas, P., Fushman, D., Ruchinsky, V. and Cowburn, D. (2000) *J. Magn. Reson.* 145, 262-275.
- Tjandra, N. and Bax, A. (1997) *J. Magn. Reson.* 124, 512-515.
- Yao, X. L. and Hong, M. (2002) *J. Am. Chem. Soc.* 124, 2730-2738.